DURABLE ICEPHOBIC COATING FOR ALUMINUM SUBSTRATE

by

Sathish Kumar Ranganathan

A Dissertation

Submitted to the Faculty of Purdue University

In Partial Fulfillment of the Requirements for the Degree of

Doctor of Philosophy

School of Materials Engineering

West Lafayette, Indiana

December 2019

THE PURDUE UNIVERSITY GRADUATE SCHOOL
STATEMENT OF DISSERTATION APPROVAL

Dr. Jeffrey Youngblood, Advisor
School of Materials Engineering
Dr. John Howarter, Co-advisor
School of Materials Engineering
Dr. Kevin Trumble, Committee Chair
School of Materials Engineering
Dr. Srinivas Siripurapu, Committee Member
Prysmian Group

Approved by:
Dr. David Bahr
Head of the Departmental Graduate Program

ACKNOWLEDGEMENTS

I would like to extend my deepest gratitude to my advisors, Prof. Jeffrey Youngblood and Prof. John Howarter for their novel ideas, constructive comments, insightful suggestions, and especially for the support provided me to balance Ph.D. work and industrial job, which have helped me to continue my research at difficult times. I am very thankful to committee chair Prof. Kevin Trumble and committee member Dr. Srinivas Siripurapu, for their valuable guidance and the great support for the past five years.

This research work would not be successful and possible without the help of General Cable (Prysmian group) colleagues and leadership team. Their support and motivation helped me to achieve the project goal and as well as thanks for their support in the lab, whenever I needed.

Finally, I would like to thank my parents, brothers, family members and friends for their support and blessings throughout my career and in the past five-years of Ph.D. duration. Special thanks to my wife Kayal for her selfless sacrifice to support my ambitions and bringing-up my sons all alone. I also would like to thank to my sons for allowing me to pursue my interest and sincere apologize for not being with them at their early childhood and fun-filled times.

This work has been supported by General Cable Corporation (Pysmian Group)

TABLE OF CONTENTS

LIST OF TABLES

LIST OF FIGURES

ABSTRACT

Author: Sathish Kumar, Ranganathan
Institution: Purdue University
Degree Received: December 2019
Title: Durable Icephobic Coating for Aluminum Substrate
Professor(s): Jeffrey Youngblood and John Howarter

Development of durable icephobic coating and reduction of ice accumulation on the product surfaces has proven to be a challenging task in the past decade. Considering the challenges posted during ice storms and existing limitations to the state of the art, development of durable icephobic coating which can provide low ice adhesion strength and less ice weight increase is a critical milestone for industries and research communities. To obtain durable icephobic coating, high temperature and weather resistance Fluoro-Ethylene-Alkyl-Vinyl-Ether (FEVE) binder was selected to design a smooth and superhydrophobic coatings. These coatings were benchmarked against commercially available silicone epoxy and superhydrophobic coatings and validated its surface roughness, surface wettability and icephobic performance such as ice adhesion strength and ice accumulation. To evaluate coatings thermal durability, targeting power transmission line application, these coatings were exposed to extreme thermal ageing conditions (200 ^{o}C for 60 days) and retention of icephobic performance were measured. Though, commercial coatings have provided better icephobicity at unaged condition, after high temperature heat ageing these coatings icephobic performance were deteriorated significantly. However, FEVE based coating had retained its surface characteristics and icephobic properties after aggressive thermal ageing.

Addition to developing icephobic coating, creating experimental understating of icephobic performance such as, the correlation between ice adhesion strength and coating material

properties also would give a great scientific knowledge and guidance to the product designers. Hence, establishing big-picture icephobic understanding can provide valuable insights to material design choices for an application, when usage of specific material or manufacturing method is not possible. For example, certain applications retaining superhydrophobic surface for longer duration would be challenging or using low modulus material is not feasible or applying highly smooth surface with zero roughness is not at manufacturing.

To map-out this design space for icephobic coating application, silicone-based coating material were selected, since silicone coating material has the flexibility to tune its properties and readily available in different modulus range as well. Silicone coatings were chosen from low modulus to higher modulus (8 psi to 28 psi) and its surface wetting properties were engineered as hydrophilic and superhydrophobic range from hydrophobic range. Also surface roughness were created using sand paper which selected with standard grit sizes such as 3000 GS, 300 GS and 30 GS. These silicone coated test panels with different mechanical properties, surface roughness and contact angles were evaluated and measured changes in ice adhesion strength. To validate ice weight increase by ice accumulation, automated ice accumulation test set-up was customized and used for icephobic performance validation. The experiment results suggest that at the lower coating modulus, roughness does not significantly affect the ice adhesion strength as compare to higher modulus coatings. Superhydrophobic coating has low ice adhesion strength across the coating modulus and roughness ranges. Additionally, superhydrophobic coatings had less ice accumulation as compare to smooth silicone coatings. Roughness plays a critical role in high modulus hydrophobic coatings, whereas smooth silicone surface performed relatively better as compare to rough surfaces.

From the experimental learnings, we have created big-picture icephobic material design space, wherein product designers can choose either hydrophobic or superhydrophobic coatings to obtain similar low ice adhesion performance, provided coatings technical attributes such as modulus and roughness are met the set requirements. From our modest literature search, we can confirm that similar material design recommendation was not made to obtain icephobic performance. Hence, we hope that researchers and industries will highly benefit from this work.

1. INTRODUCTION

1.1 Background and motivation

In the past decade, ice-phobic coating research has attracted academic and industrial research interest [1-8]. The primary reason for this increased attention was to increase human safety and durability of the products during ice storms. Ice accumulation can create hazardous conditions on structures, roads, bridges, towers, buildings, and energy application products [9-13]. Multiple research studies have reported that hydrophobic and superhydrophobic surfaces could enhance ice-phobic performance [14-19]. Additionally, these surfaces have potential to improve dust resistance, corrosion resistance and marine fouling resistance [20-25]. These coatings are manufactured with various coating process techniques such as metal surface etching, plasma deposition, chemical deposition, vapor deposition and single step immersion coating [26-35]. To obtain a commercially successful coating product, an icephobic coating surface should have long term durability and easy manufacturability with commoditized methods are critically important.

Extensive studies were performed in this regard have proved that for producing surfaces with low ice adhesion strength and reduced ice accumulation, the coated surface should have the following characteristics: low surface energy, high contact angle, reduced surface roughness, and low elastic modulus [36-53]. To validate these parameters to icephobicity numerous studies have been conducted by researchers.

Meuler et al. [54] demonstrated the relationship between ice adhesion strength and contact angle hysteresis (CAH) to validate the role of hysteresis to icephobicity. Oberli et al. [55] reported a correlation between ice adhesion strength and surface free energy; they both have analyzed the role of the contact angle in ice adhesion and reported that superhydrophobic surfaces can provide low ice adhesion. At the same time, other approaches such as, altering surface lubrication and

interfacial slippage have also been considered. Aizenberg [8] developed a novel liquid-infused porous material that can produce significant slipperiness and provide extremely low ice adhesion and anti-ice performance. Golovin [39] measured ice adhesion values of a silicone coating material (SylGard 184) by altering its interfacial slippage and hardness properties. He had varied the curing conditions by changing the curing temperature and time from 150°C/24 h to 80°C/2 h and lowered the ice adhesion strength from 245 KPa to 36 KPa. The changing curing conditions helped to increase the interfacial slippage and reduce the modulus of the coating. Similarly, Zhang et al. [51] prepared a low-modulus silicone material and achieved lower ice adhesion strength. In another work, Beemer et al. [47] also observed that polydimethylsiloxane (PDMS) coatings with low shear modulus has resulted in reduced ice adhesion strength. However, altering the shear modulus in the further lower ranges from 1 psi to 22 psi, did not change the ice adhesion strength significantly. He also tested the durability of the PDMS coating by subjecting coatings to 1000 abrasion cycles using 400 grit sandpaper. These abrasion cycles increased the coating RMS roughness from 0.05 μm to 3.52 μm. However, only a small increase in ice adhesion strength (< 2 KPa) was observed, while the roughness was increased significantly. This finding is contrast with other studies which has reported that increased surface roughness led to significant increases in ice adhesion strength. In another work, Zou [49] evaluated a silicone-doped hydrocarbon and substrates coated with a fluorinated-carbon polymer by altering the RMS roughness from 0.3 to 2.49 microns by sandblasting. He observed that ice adhesion strength increased to more than 100 KPa with the increase in roughness. Similarly, Markus Susoff [46] reported that increases in roughness led to ice adhesion strength higher than 50 KPa, it can be inferred that there are three key parameters that influence ice adhesion strength. They are the surface tension and wettability of the coating, roughness of the coating surfaces, and mechanical properties of the materials. These

inferences are in line with theoretical relationships established by researchers. Gao et al. [56] analyzed ice adhesion strength using practical work of adhesion (Wp) describing the relationship using surface tension and receding contact angle with following equation (1): $Wp = \gamma_{LV} (1+ \cos \theta rec)$, where γ_{LV} is the surface tension at the liquid–vapor interface and θrec is the water receding contact angle of the coatings. To understand role of surface roughness to the ice adhesion strength, Zou et al. [57] explained the relationship between surface roughness and ice adhesion strength. The ice adhesion stress (τ) can be calculated by measuring the force (F) required for removing ice from the ice contact area (A) on the test substrate, using the following equation (2): $\tau = F/A$. The third parameter influencing ice adhesion strength is the coating modulus. The role of the coating modulus and its relationship with ice adhesion was elaborated by Kendall [58] and Griffith [59]. The force required to remove ice from the substrate is calculated by using the following equation (3): $\tau_{ice} = \sqrt{\frac{Wa\mu}{t}}$, here, τ_{ice} is shear stress, Wa is the work of adhesion between substrate and ice, μ is shear modulus and t is thickness of the coatings material. Other researchers, Baier [60] and Vladkova [61] have elaborated mechanism of adhesion force by analyzing the combined role of surface energy and elastic modulus, rather than considering each of them separately, and considered following relationship (4): $(\gamma c.E)^{1/2}$, whereas, γc is critical surface energy and E is elastic modulus of the coating.

Above mentioned studied suggest that to obtain low ice adhesion and reduced accumulation surface, coating should have higher contact angle, less roughness and low elastic modulus. Having said that to have a commercially successful icephobic product, the developed coating should have to meet product application and durability requirements. Hence validating coating durability performance is highly critical for commercial applications. Durability of ice-

phobic coating performance studied using various environmental factors such as ultraviolet (UV) radiation, mechanical abrasion, thermal cycling, humidity variations and other ageing conditions [60-64]. Vedder et al. [39] studied retention of ice-phobic properties by exposing the coated samples to a combination of UV radiation, salt spray, mechanical abrasion and thermal ageing test conditions up to 7 days. Similarly, Chao Tao et al. [40] reported that fluorinated POSS hybrid coatings exhibited durable low ice adhesion properties even after 15 de-icing cycles. However, these studies have demonstrated only short-term durability of coatings. However, there is a significant importance to understanding durability of ice-phobic coatings during longer service conditions to simulate exterior product performance for the lifetime of the product. Future work in this area should focus on understanding the combined role of coating formulation, ice-phobic performance and ice-phobic performance retention over extreme conditions and time-scales. The ideal ice-phobic coating should be environmentally friendly, able to be integrated into industrial scale manufacturing processes and be able to maintain high performance during the lifetime of the product. Hence, we have selected water-based fluoroethylene vinyl ether (FEVE) dispersion coating which has the proven track record long-term exterior durability performance [65-68]. FEVE based coating formulation were benchmarked against commercially available coatings to validate its icephobic durability at extreme thermal conditions.

Additionally, as part of this research work, the icephobic research learnings need to be scientifically established for broader applications, hence we considered silicone materials, which is relatively easy to engineer its properties and commercially available with various elastic modulus levels. These material silicone material is selected to establish ice adhesion correlation with roughness, modulus and contact angle.

1.2 Research Objectives

The objective of this research work is to create an understanding of icephobicity for industrial application and as well to develop a durable icephobic coating which can be applied to power transmission products and other applications.

1) Develop a water based or low VOC coating formulation with improved icephobic properties such as low ice adhesion and ice accumulation. Also study the thermal durability of the developed coating, which is critical for power transmission products which are operated at relatively high temperatures like 100^{o}C to 200^{o}C.
2) Establish a broader design space for icephobic surfaces, to understand the relationship between roughness, modulus and water contact angle to ice adhesion strength, by utilizing these learnings, product designers can have options to choose either hydrophobic or superhydrophobic coating to achieve similar low ice adhesion results.
3) Validate ice accumulation performance of coatings with different modulus and contact angles, also validate sample placement angle against water spray direction, to understand the role of product design in ice accumulation.

1.3 Overview of This Work

In this research work, development of durable icephobic coating for aluminum substrate, establish a scientific understanding to achieve a low ice adhesion strength and evaluating different coatings ice accumulation weight increase was focused. Ice adhesion and ice accumulation test method was developed to validate icephobic performance of the coatings. Silicone coating material was selected to establish icephobic influencing parameters and FEVE based coating material was selected to validate high temperature durability of icephobic performance.

High speed lab mixer was used to mix coating ingredients, brush application was used to prepare coated test panels. Aluminum thin sheet (30 mil thickness) was used as substrate. Scanning electron microscope (SEM) were used for surface and morphological analysis. Contact profile-meter was used to measure surface roughness, Instron tester coupled with cold chamber was used to measure ice adhesion strength. Cold chamber with water spray and automated ice weight measurement method was used to measure ice weight measurement.

Chapter 2 describes the materials and methods used for this research work to prepare a coated test panels for water contact angle measurement, surface roughness and surface topography analysis. Also, we reported here the in-house test method which was used to validate ice adhesion strength and ice accumulation weight increase.

Chapter 3 covers FEVE binder coating formulation development and comparison with commercially available smooth and superhydrophobic coatings. The surface properties such as roughness, contact angles and icephobic properties such as ice adhesion and ice accumulation were measured. Thermal durability of the coatings was evaluated at 200 ^{o}C by exposing coated test panels for 60 days.

Chapter 4 elaborates the role of silicone coating material influencing factors to ice adhesion strength. The elastic modulus, surface roughness and water contact angles were varied and evaluated its influence on ice adhesion strength. Finally, we created icephobic material selection design space for future research and product development.

Chapter 5 discuss the ice accumulation test data of silicone coatings by comparing: 1) low and high modulus silicone coatings (smooth surface) and 2) hydrophilic, hydrophobic and superhydrophobic coatings. 3) Additionally, superhydrophobic coated panels, test placement angle was varied against water spray direction and ice weight increment was calculated

Chapter 6 is the summary of research work and discuss about the experimental findings and recommendation for future industrial and commercial use.

2. MATERIAL SELECTION AND TEST METHODS

All lab-work in this chapter was performed by Sathish Kumar Ranganathan. All data analysis was performed by Sathish Kumar Ranganathan with guidance by Prof. Jeffrey P. Youngblood and John Howarter. All writing was performed by Sathish Kumar Ranganathan with guidance and editing by Prof. Jeffrey P. Youngblood and John Howarter.

2.1 Introduction

Durability of icephobic coating performance were validated by researchers using various environmental factors such as ultraviolet (UV) radiation, mechanical abrasion, thermal cycling, humidity variations and other ageing conditions [60-64]. However, these validations are limited with time scale and temperature. Considering power transmission application requirement, we have chosen 200^{o} C temperature condition for ageing test panel and validated its icephobic performance, especially after 60 days of heat ageing. Additionally, FEVE binder-based coating has proven track record of exterior product lifetime more than 30-40 years. Hence, we designed FEVE based coating formulation and compared against commercially available aerosol superhydrophobic coating and smooth silicone epoxy coatings.

2.2 Materials Selection

2.2.1 Fluoro-Ethylene-Alkyl-Vinyl-Ether (FEVE) binder selection

The ideal icephobic coating should be environmentally friendly, able to be integrated into industrial scale manufacturing processes and be able to maintain high performance during the lifetime of the product. FEVE as a binder in coating formulations with a suitable crosslinker, provides long term UV stability, hydrolytic and thermal stability as demonstrated by previous researchers. The chemical structure of FEVE binder is disclosed in figure 2.1 [67-71]

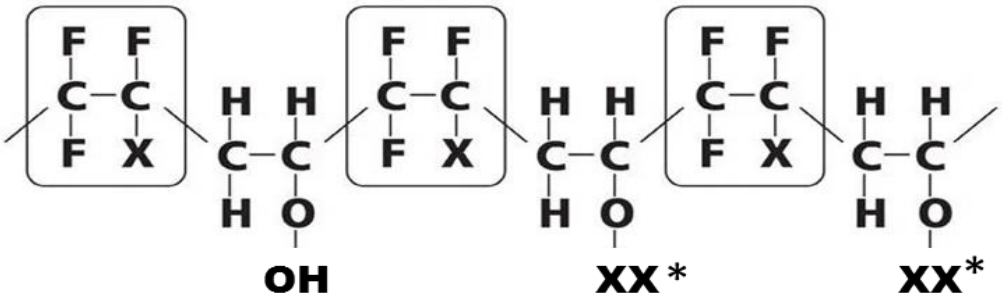

Figure 2.1. Chemical Structure of Fluoro-Ethylene-Alkyl-Vinyl-Ether (FEVE),

(* Chemical structure or polymer branch is proprietary to the supplier)

Water-based fluoroethylene vinyl ether (FEVE) dispersion is a base for coating formulations and its properties were engineered using appropriate coating additives and along with silica filler to obtain a smooth and modified rough coating. Also, to evaluate a thermal durability the developed coating formulation, coated test panels were further aged at high temperature and compared its icephobic properties against commercially available coatings. The more details about coating mixing, sample preparation and test data will be discussed in the following chapter.

2.2.2 Silicone coating material selection

To understand the role of coating material characteristics and its influences on the ice adhesion strength, Poly-Dimethyl-Siloxane (PDMS) based silicone coating material were selected [72-75]. The selected silicone coating was purchased from Smoothsil LLC and used to prepare coated test panels at the lab. The cured silicone coating material surface is hydrophobic and to develop a hydrophilic surface PDMS-glycol additive were mixed with silicone coating and to prepare superhydrophobic surface commercially available fluorosilane aerosol coating

(Waterbeader) was sprayed on the silicone cured test panel. The further details about material mixing and procedure will be discussed in chapter 4.

2.3 Analytical methods

Quantifying the icephobic performance of the coatings is important to understand commercial feasibility of developed coating compositions. The most common way to achieve icephobic surfaces is by eliminating water from the surface as quickly as possible before the water becomes static and nucleates ice crystals. By quickly removing the water, water-substrate contact time is reduced, which helps to minimize the ice nucleation rate and can delay ice layer formation and ice growth [28-30]. Once ice has accumulated on the coated substrate, the ice can be removed by its own weight or by external forces such as wind or vibrations [76-79]. To achieve effective ice removal, functional coatings should have reduced ice adhesion force, so that minimal ice weight or minor external forces are sufficient to remove or eliminate the ice from the surface. Considering all these technical requirements, the potential icephobic coating should have hydrophobic properties with lower water sliding angle leading to less total ice accumulation and reduced ice adhesion force. To validate these critical performance characteristics of the selected coatings, surface roughness was measured, scanning electron microscope (SEM) imaging were used to image surface roughness and morphology, water contact angle and water sliding angle measurement test method were used to evaluate hydrophobicity, a custom designed ice chamber outfitted on a mechanical load frame (Instron) was used to measure ice adhesion force and a custom designed ice accumulation chamber for in-situ ice accumulation weight measurement

2.3.1 Surface roughness measurement

The surface characteristics of the coated aluminum test panels were analyzed to understand the influence of surface roughness on the ice-phobic performance. The Ra and Rz roughness values were using Mahr PS1 digital contact profile meter on five different locations of the same test panel. Ra roughness is calculated by averaging peaks and valleys of the roughness profile. Rz is calculated by measuring the highest peak to the lowest valley within a sampling area by averaging these distances. Rz averages only the five highest peaks and the five deepest valleys. Hence most Rz values are larger than Ra roughness values [80]. Superhydrophobic coatings which exhibits large Rz values would be beneficial to create nanoscale air pockets which facilitates Cassie Baxter surfaces [81]. To further characterize coating surface morphology, SEM images were captured using a Topcon-300 instrument at 30KV and 100X magnifications.

2.3.2 Water contact and sliding angle measurement

The surface wetting properties such as advancing, receding and water sliding angles were measured at room temperature. The water contact angle measurements were carried out using a 10µl water drop. The advanced and receded contact were measured, by enlarging and shrinking the water droplet, respectively, via a metal needle from a manually operated syringe. A Dino-lite digital microscope analyzer was used to calculate the advancing and receding contact angles. The water sliding angle of coated test panels were measured by carefully placing a 10µl water drop on a test panel that was then slowly tilted to initiate water movement. The angle at which the water has started rolling-off was measured as water sliding angle and captured through digital image software. Five data points were captured at different locations of the same test panel and the average value is reported. The surface wetting parameters and surface morphology

characterization were measured before and after heat exposure to validate the durability of coating and to understand influence of heat ageing of the ice-phobic performance results.

2.3.3 Mechanical properties measurement

The hardness of the silicone materials was measured using a hand-held shore A hardness meter; the indenter was pressed against surface of the rubber and the displayed hardness value was noted. The elastic moduli (E) of precut rubber samples (1 inch * 5 inch* 45 mil) were measured using a Zwick 1455 universal testing machine at 0.2 inch per minute test speed. The average values of three measurements were recorded as the elastic moduli of the various coating materials.

2.3.4 Ice adhesion strength measurement

The ice adhesion strength was measured by applying a pull shear stress to an ice cylinder which was adhered on a coated test panel. The test set-up schematic is represented in the figure 2.2. Previously, to form the ice cylinder on coated test panel, water filled cylindrical container was positioned on the coated test panel surface at -10 ^{o}C for 24 hours. The dimensions of the cylindrical container dimensions are 3 inches in diameter and 2 inches in height. After ice was formed on coated test panel, ice cylinder along with coated test panel were hooked with Zwick 1455 tensile test instrument to measure adhesion force. The ice adhesion test was conducted inside a cold chamber which was maintained -10 ^{o}C and at least five tests were done to calculate an average ice adhesion strength.

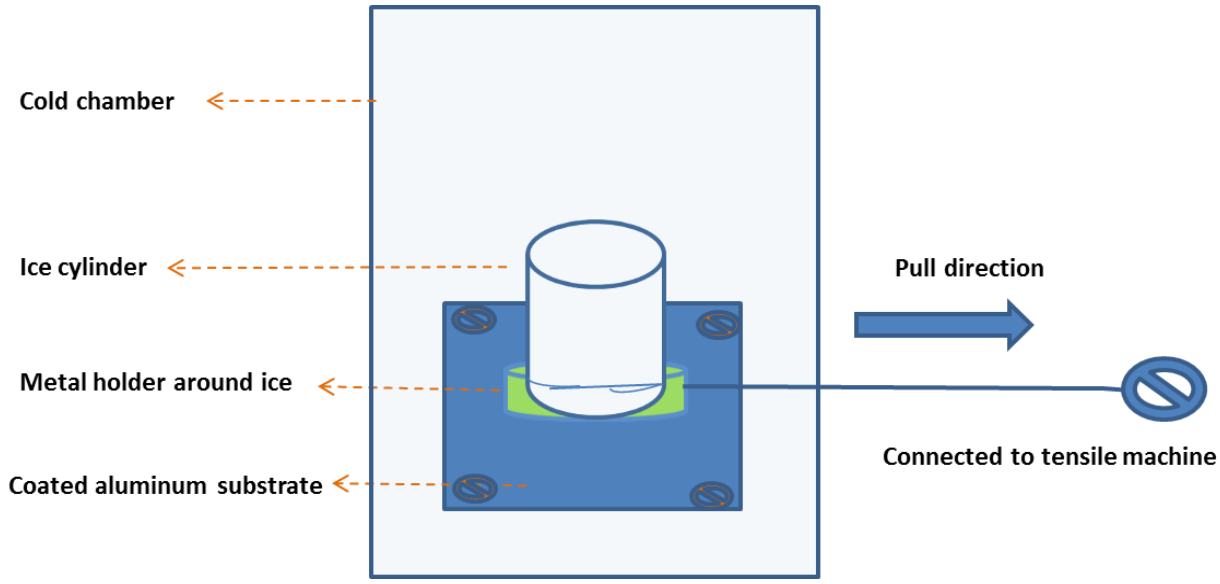

Figure 2.2. Schematic representation of ice adhesion strength test set-up

2.3.5 Ice accumulation test method

The ice accumulation test was conducted inside a cold chamber, where the test temperature was set as -10 ^{o}C and precooled water (at 4 ^{o}C) was sprayed through an array of water misting nozzles. The test set-up schematic is represented in the figure 2.3. The water pipe pressure was maintained at 40 psi, the distance between the test panel and water mist nozzle was maintained about 50 inches. The ice accumulation test lasted for duration of 60 minutes of water spray and the weight of the test panels were measured continuously during ice accretion process and reported as ice weight increase.

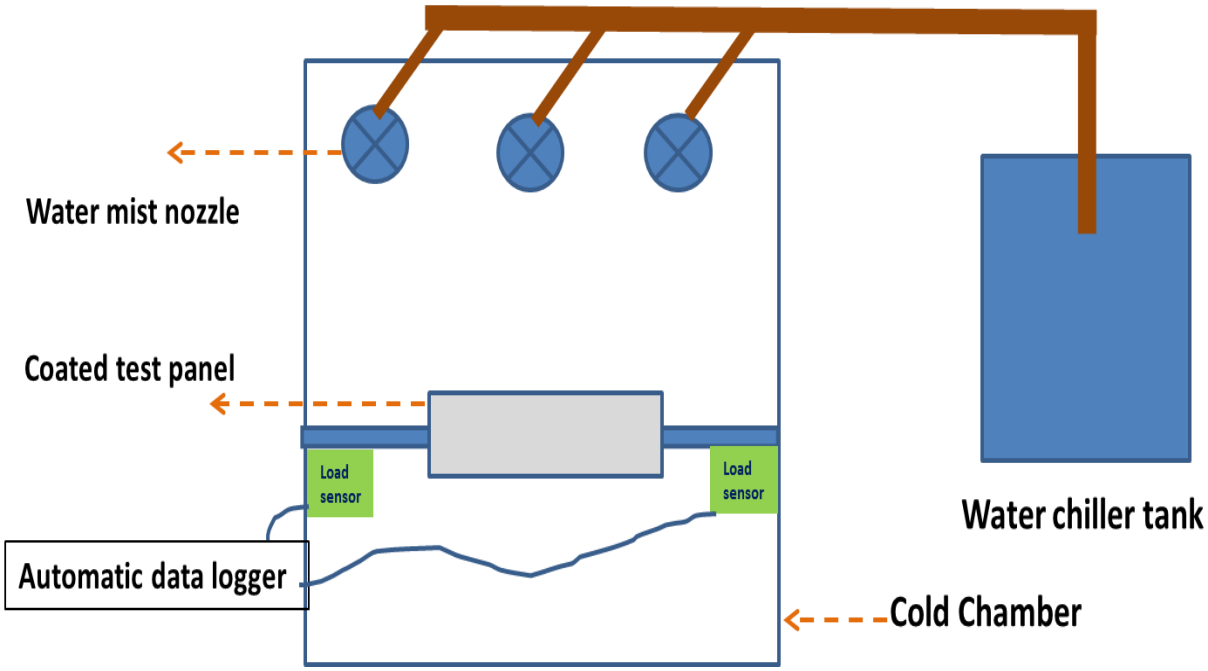

Figure 2.3. Schematic representation of automated ice accumulation measurement set-up

3. FEVE COATINGS ICEPHOBIC AND THERMAL DURABILITY VALIDATION

3.1 Introduction

We report here design of new coating formulations using FEVE with crosslinking agents with functional additives to control surface properties. We compare the new coatings with commercially available coatings such as silicone-epoxy coating and fluorosilane aerosol coating. To understand thermal and long-term performance of these applications, coated test panels were aged at 200 ^{o}C and up to 60 days. At frequent thermal ageing intervals, both static and rolling water contact angle were measured. Other properties such as surface roughness, ice adhesion, ice accumulation was measured before and after thermal ageing exposure. We hypothesize that use of a binder such as FEVE with proven exterior and thermal performance characteristics will provide high temperature stability of the resultant coating and that silica addition will positively impact on ice-phobic performance.

3.2 Material and methods

3.2.1 Coating materials

To develop FEVE based coating formulations, commercially available coating fillers and additives were obtained. Lumiflon FD1000 is a water based FEVE dispersion received from AGC Chemicals Americas, Exton, PA. The datasheet provided by manufacturer indicates 40 weights percent solid content with a hydroxyl value of 85 mg KOH/g-polymer. The cross-linker was received from Covestro (formerly Bayer material science), located at Leverkusen, Germany. The cross-linker trade name is Bayhydhur BL 5335, which is a water dispersible blocked aliphatic polyisocyanate with a blocked NCO content of about 7.1 weight percent. The total non-volatile

content of crosslinker is 34 to 36 weight percent. Nano silica material was received from Cabot, Billerica, MA., under the trade name of CAB-O-SIL® TS-720. This silica has a surface treatment of dimethyl siloxane with the B.E.T. surface area of 200 m^2/g and specific gravity of 2.2 g/cm^3. The FEVE dispersion was mixed with cross-linker at a weight ratio of 90:10 to produce smooth fluoropolymer coating. Silica-filled fluoro coating was produced by mixing FEVE dispersion, cross-linker and treated silica with a weight ratio of 87.5:10:2.5. Other coating additives like defoamers, leveling agents and dispersion aids were added at 0.25 weight percent in the both coating formulations.

A proprietary silicone-epoxy coating and solvent based two-layer fluorosilane aerosol coating (commercial name: Neverwet) were purchased as comparative samples. Silicone-epoxy coating part-a is comprised of silicone epoxy with a 53-weight percent solid content; part-b is amino cross-linking agent with 46 weight percent solid content. To obtain a silicone epoxy coating the part-a binder and part-b cross-linker were mixed at 80:20 weight ratio. The solvent based fluorosilane aerosol coating was prepared by applying the silica modified epoxy-based primer as base layer followed by fluorosilane top layer by spray deposition method to obtain a two-layer fluorosilane aerosol coating. These coating materials were used to prepare coated aluminum test panels for further test and validation.

3.2.2 Coating mixing and test panel preparation

A coating mixing and test panel preparation schematic is shown in figure 3.1. For this research four different coating formulations were examined. Three coatings which were made with a single layer deposition and will be referred as 1) smooth fluoro coating, 2) silicone epoxy coating and 3) silica-filled fluoro coating were prepared in two steps. The fourth two-layer coating will be referred as fluorosilane aerosol coating which was prepared by two steps spray method.

To deposit a single layer coating formulation, the coating ingredients were mixed and stirred vigorously at 1000 rpm for 15 minutes using a high-speed mixer to obtain a uniform dispersion. The dispersion was applied using a foam brush to the prepared aluminum panels and panels cured at 150 ^{o}C for five minutes. The two-layer fluorosilane aerosol coating and its epoxy primer were supplied in separate pressurized metal containers.

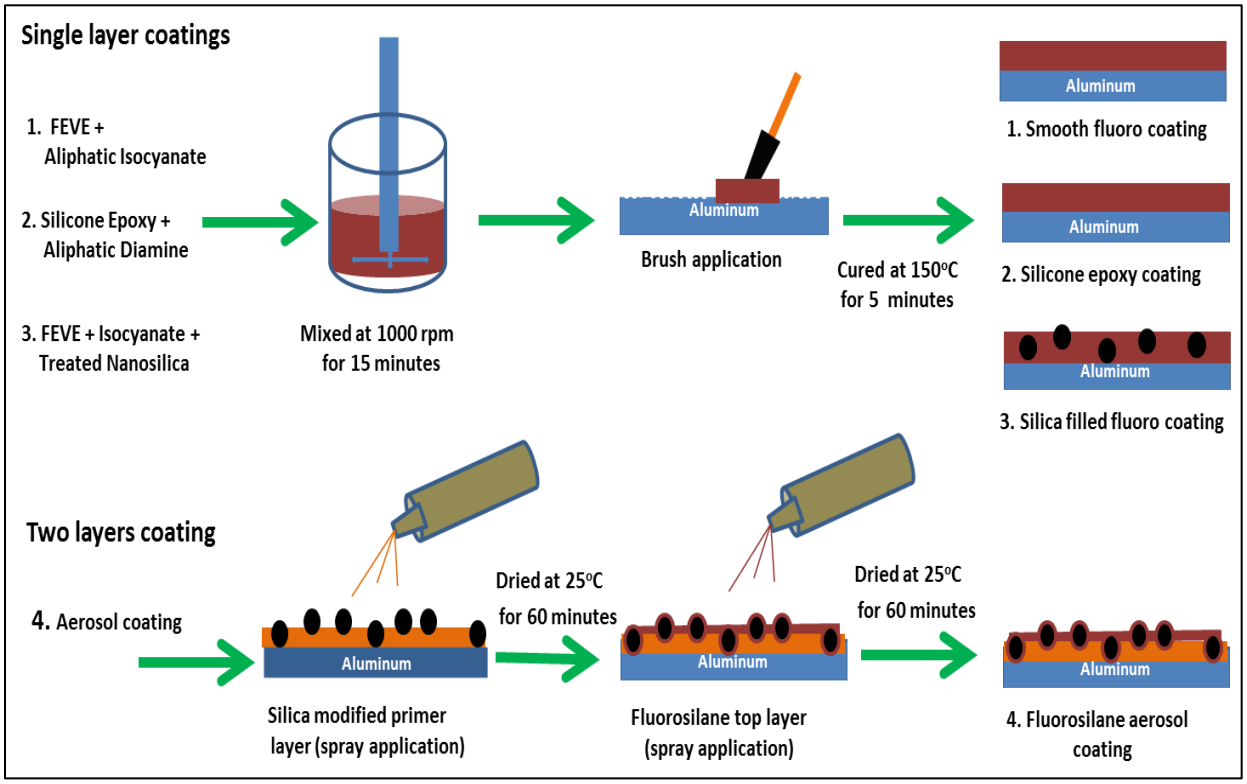

Figure 3.1. Schematic representation of coated test panel preparation steps.

To prepare aerosol coating, each material (primer and top layer) were separately sprayed on the aluminum test panel and a 12-inch distance was maintained from container spray tip towards the aluminum panel to achieve a uniform surface finish. Firstly, inner layer primer was applied and dried at room temperature for one-hour. Later, the top layer was applied and allowed to dry at room temperature.

3.3 Result and discussion

The icephobic performance of coated test panels were characterized before and after heat ageing exposure to understand its durability and retention of roughness, ice adhesion force and ice accumulation properties. The test results and its technical details are discussed further.

3.3.1 Surface topography analysis

SEM images of the unaged and heat-aged (60 days at 200^{o}C) coated test panels are shown in figure 3.2. From the qualitative observation, the surface roughness of the smooth fluoro polymer coating was not changed significantly after heat exposure, whereas silicone epoxy coating surface developed a rippled surface texture. The increase rippled surface was possibly due to wrinkling of the coating [82].

The silica-filled fluoropolymer coating surface had finer peaks and valleys after heat ageing as compared to the unaged surface. The two-layer fluorosilane aerosol coating surface morphology has qualitatively changed after heat ageing with increased gaps and reduced roughness peaks. To quantify and understand further these surface morphology changes, surface roughness measurement was made on coated test panels using a contact profilometer. The measured roughness results are shown in table 2.1. All three single layer coatings were resulted in increased Ra and Rz roughness after heat ageing exposure. Notably, the two-layer fluorosilane aerosol had reduced roughness in both Ra and Rz after heat ageing. Similar observation was made on SEM image of fluorosilane aerosol coating, which was exhibited large equiaxed features before

heating and a qualitatively smoother surface after heat ageing. It is possible that the underlying primer layer had degraded during the high temperature heat exposure [61 and 82].

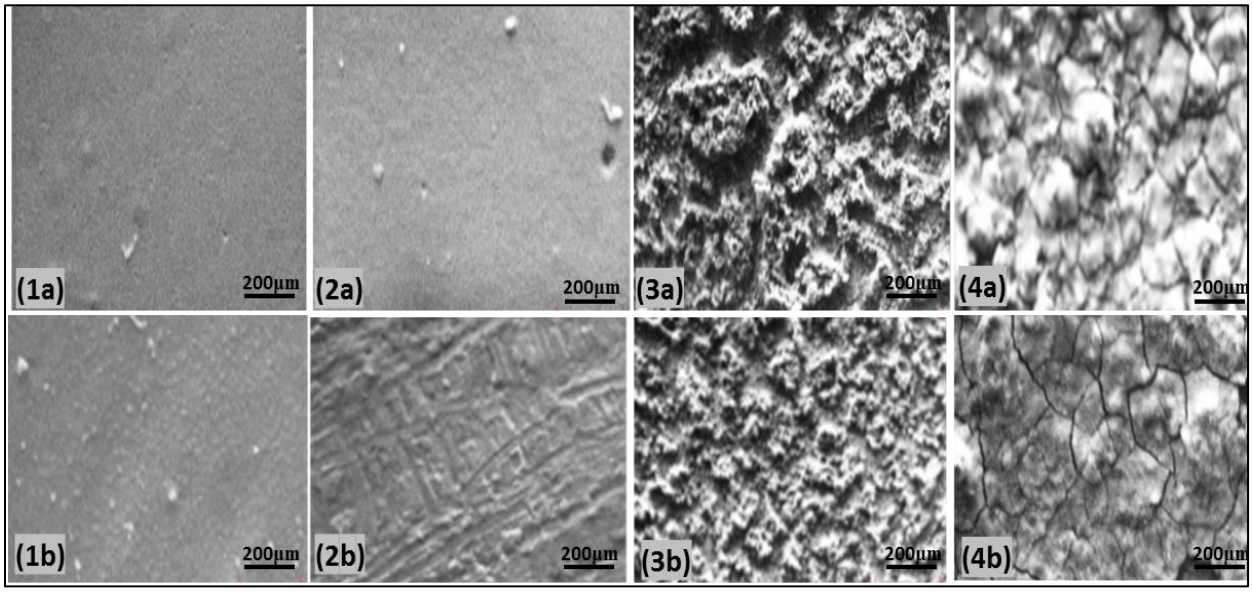

Figure 3.2. SEM images of the unaged (top images) and heat aged (bottom images) coated test panels for 200°C for 60 days; (1a & 1b) smooth fluoro coating, (2a & 2b) silicone epoxy coating, (3a & 3b) silica-filled flour coating and (4a & 4b) fluorosilane aerosol coating.

Table 3.1. Sample description and surface roughness of Ra and Rz properties. The change in roughness is calculated and reported as % change

Sl.no	Coatings	Roughness, Ra (µm)			Roughness, Rz (µm)		
		Before ageing	After ageing	% Change	Before ageing	After ageing	% Change
1	Smooth fluoro coating	6.1 ± 0.4	7.9 ± 0.5	29.5	6.7 ± 0.8	7.5 ± 1.2	11.9
2	Silicone epoxy coating	8.8 ± 0.7	10.2 ± 0.9	15.9	8.5 ± 0.6	10.6 ± 0.9	24.7
3	Silica filled fluoro coating	11.1 ± 1.1	13.2 ± 1.2	18.9	51.4 ± 4.2	56.7 ± 2.8	10.3
4	Fluorosilane aerosol coating	3.8 ± 0.2	1.8 ± 0.1	-52.6	25.5 ± 1.6	9.2 ± 3.8	-63.9

3.3.2 Surface wetting properties

The early step of the icing process is surface wetting, wherein a water drops contacts with the substrate surface, which is followed by ice nucleation and freezing. To understand surface wetting performance of coated surfaces, dynamic water contact angles and water sliding angles

were measured during heat ageing using 10µl water drop size. The summary of water advancing, and receding contact angles are reported in figure 3.3 a & b.

Initial water advancing contact angles of smooth fluoro coating and silicone epoxy coating were similar within the hydrophobic range of about 100^{o}, whereas silica-filled fluoro coating and fluorosilane aerosol coating was closer to the superhydrophobic range of about 138^{o} & 151^{o} respectively. This initial advancing contact angle data aligns with surface roughness measurement, whereas the smooth fluoro polymer coating and silicone epoxy coating both resulted a smoother surface than the silica-filled fluoro coating and fluorosilane aerosol coatings.

It is important to note that the smooth fluoro coating and silica-filled fluoro coating used the same FEVE dispersion and crosslinker. The addition of silica filler in the later coating creates the surface roughness and thus contributes to the increase in advanced contact angle. This observation validates surface wetting concepts of the Wenzel and Cassie-Baxter models which suggest that rougher surfaces bring higher contact angles for hydrophobic surfaces than smoother coating surfaces [81].

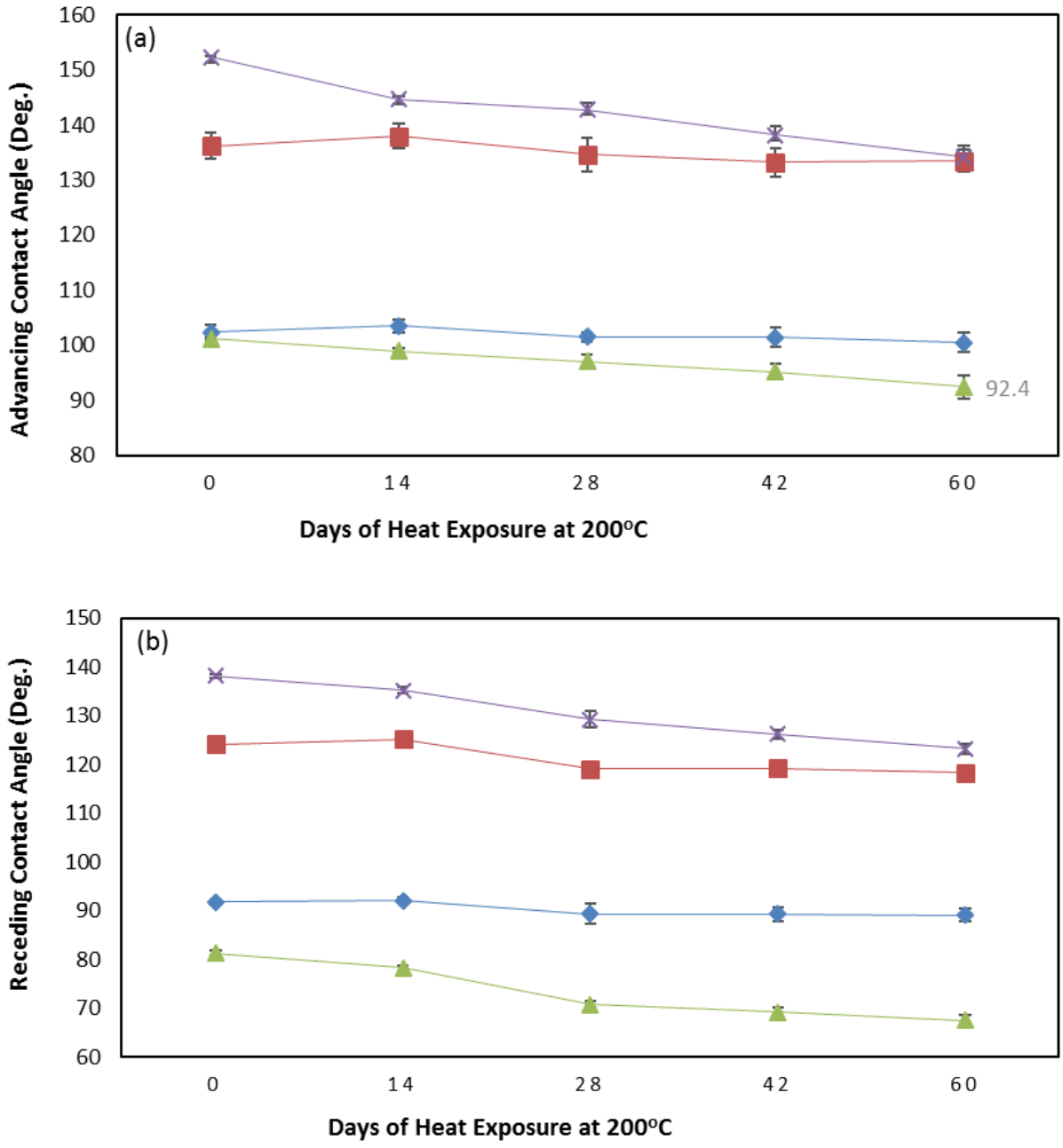

Figure 3.3. Water contact angle test data of coated test panels. (a) advancing contact angle and (b) receding contact angle. ◆ smooth fluoro coating, ▲ silicone epoxy coating, ■ silica-filled fluoro coating and x fluorosilane aerosol coating

The water contact angle hysteresis (CAH) and sliding angles can provide additional information about water wetting behavior and values are reported in figure 3.4 a & b. The contact angle hysteresis of silicone epoxy coating was observed to be an outlier (CAH = 20^o) as compared to the other three coatings and the same CAH trend (ranges between 10^o to 15^o) observed after heat aging as well. The water sliding angle of the smooth fluoro coating, silicone epoxy coating, and silica-filled fluoro coating were similar at about 10^o, whereas the fluorosilane aerosol coating sliding angle was significantly low at 2^o. This was primarily due to the higher advancing contact angle and low CAH induced by the surface roughness. However, the water sliding angle of the fluorosilane aerosol coating was increased multifold to 10^o after heat exposure.

As the observed surface roughness of this coating had changed significantly after heat ageing, this likely had the impact of increasing sliding angle. Interestingly, the sliding angle of smooth fluoro coatings and silica-filled fluoro coatings were also the same as with fluorosilane aerosol coating sliding angle at 10^o after heat exposure, thus heat treatment had the effect of equalizing these coatings. This result confirms that two-layer fluorosilane aerosol coating does not have high thermal degradation resistance at high temperature, whereas FEVE dispersion coatings retains surface properties. Like the fluorosilane aerosol coating, silicone epoxy coatings also were not able to retain surface properties and hence the sliding angle of this coating increased significantly (30^o) after heat ageing to become the highest of all the coatings.

The unaged surface topography and surface wetting property results of unaged coatings test data suggest that fluorosilane aerosol coating and silica-filled fluoro coating has high potential to give good icephobicity performance due to higher advancing contact angle and low sliding angles. However, after heat exposure FEVE dispersion coatings retain surface properties, hence we could anticipate that these coatings would have durable ice-phobic performance after heat

ageing. To validate this observation, icephobicity tests such as ice adhesion and ice accumulation were conducted with all coated specimens before and after heat ageing.

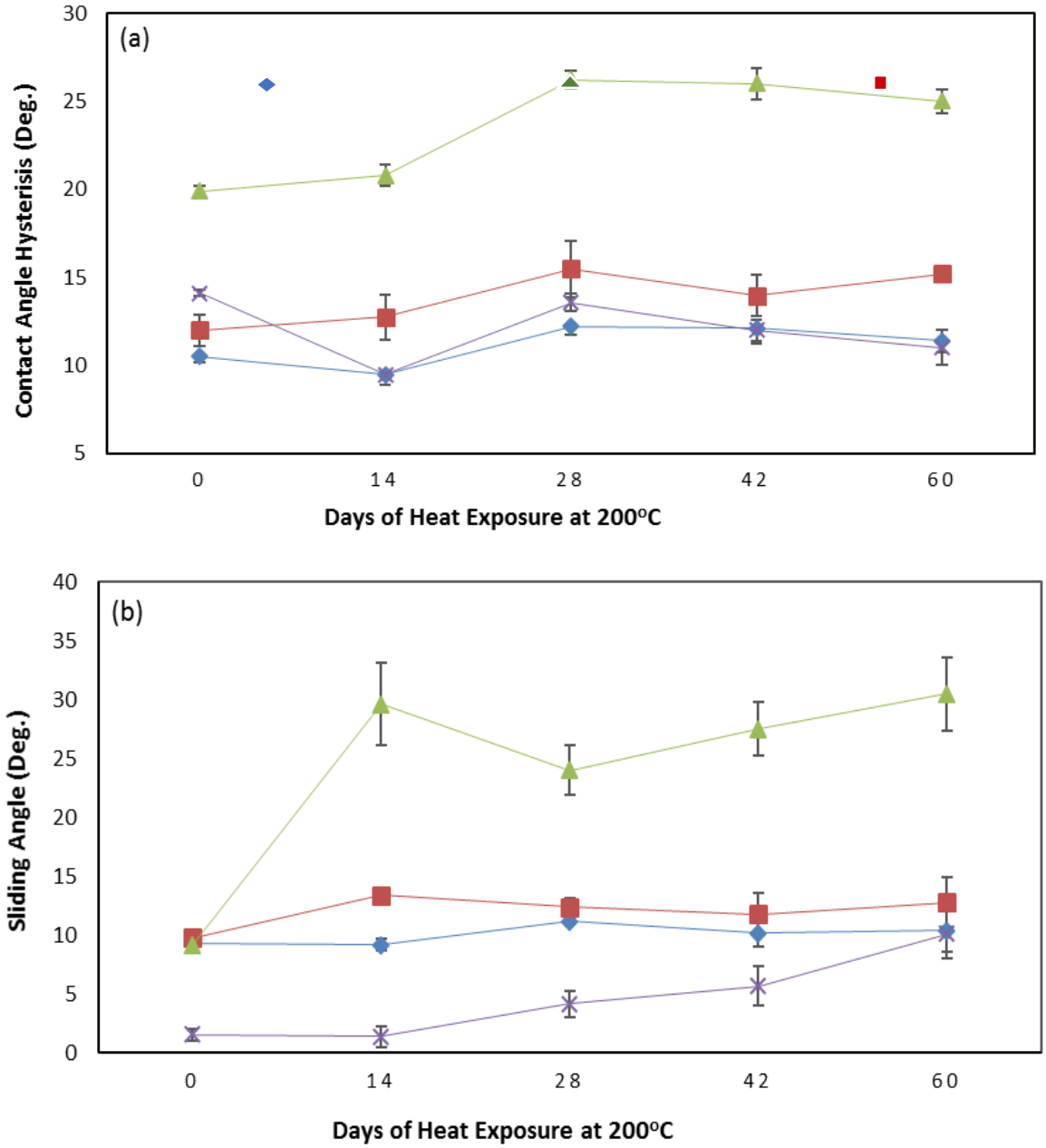

Figure 3.4. Water contact angle test data of coated test panels. (a) contact angle hysteresis and (b) water sliding angle.◆smooth fluoro coating,▲ silicone epoxy coating,■ silica-filled fluoro coating and x fluorosilane aerosol coating

3.3.3 Icephobic properties

To understand the influence of surface topography and wetting properties on the icephobicity performance, ice accumulation and ice adhesion tests were conducted. The ice accumulation weight increase was measured by placing coated test panels vertically inside the cold chamber. Before starting the test, coated panels were kept for one hour to obtain a uniform temperature (-10 ^{o}C) of the freezer and test panel. The test panel weights were measured physically before and after the ice accumulation test. The image of the test panels after the ice accumulation test is shown in figure 3.5. The increase in ice weight percentage of both unaged and heat aged (200 ^{o}C for 60 days) is reported at the bottom of each test panel image.

The ice accumulation weight increase on an unaged test panel of smooth fluoro coating, silicone epoxy coating and fluorosilane aerosol coating showed less ice weight (<10 weight %), whereas the silica-filled coating showed a slightly higher ice weight accumulation (>10 weight %) than the earlier mentioned coatings. The superhydrophobic coating can delay ice nucleation and ice formation due to its low contact area on the substrate and also can remove water from substrate surface faster, due to its low sliding angle, hence it has resulted in less ice accumulation [7-12]. And as compare to smooth fluoro coating and silica filled coating had high Ra and Rz roughness which had contributed in increased ice accumulation [6,42 and 66]

After thermal exposure, ice weight increase of a silicone epoxy coating was increased multifold from 5.2% to 28.2%. Silica-filled fluoro coating and fluorosilane aerosol coating ice weight was doubled when compared to before and after heat ageing. Interestingly, the smooth fluoro coating maintained a similar ice weight, when compared to the unaged test panel. FEVE

binder has better thermal ageing resistance as compare to fluorosilane and silicone epoxy coatings, hence, it helped to retain its surface properties [67-69].

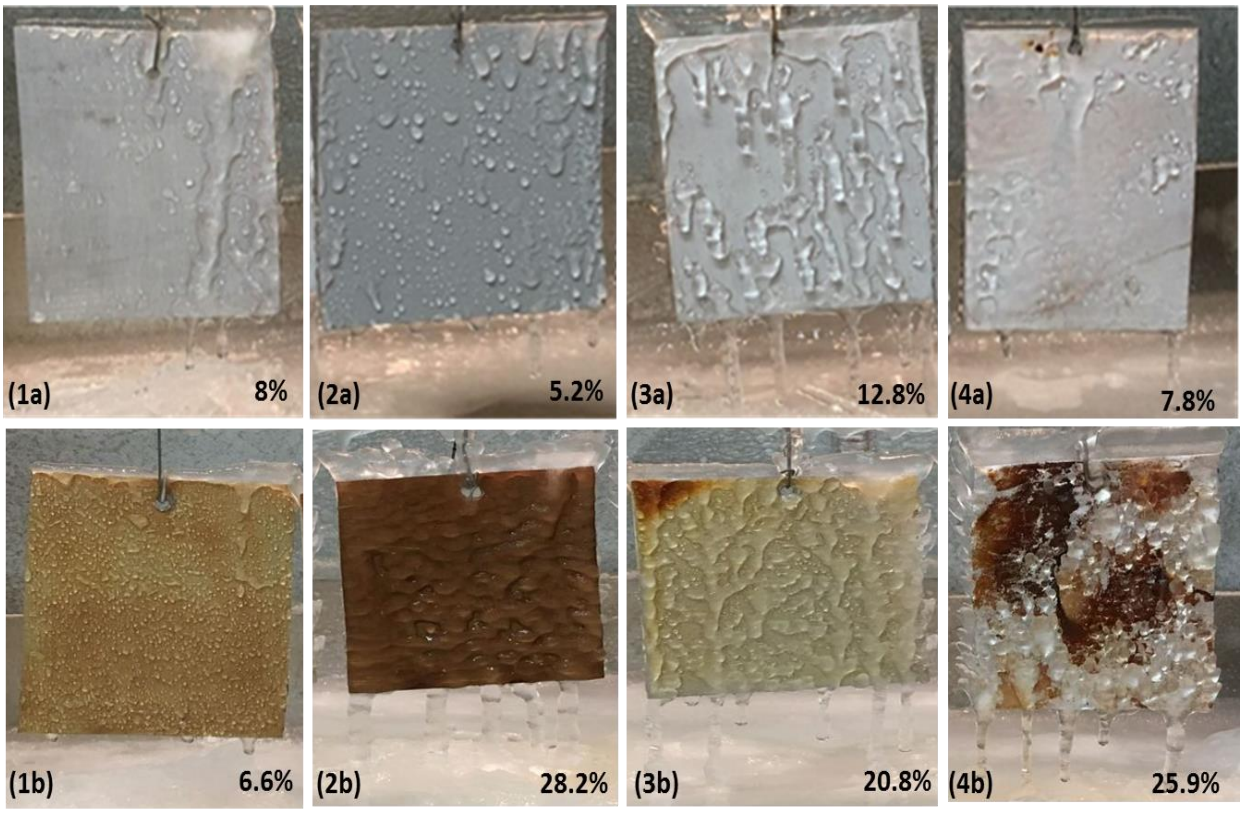

Figure 3.5 Ice accumulation test images of the unaged and heat aged test panels. (1a & 1b) smooth fluoro coating, (2a & 2b) silicone epoxy coating, (3a & 3b) silica-filled fluoro coating and (4a & 4b) fluoro silane aerosol coating.

After heat ageing aerosol superhydrophobic coating icephobic performance were affected significantly, this outcome could be due the fact that smooth fluoro coating has reduced roughness as compare superhydrophobic coating, which had an increased roughness due to thermal degradation [27 and 63]. The test panels used in the ice accumulation test were placed vertically and water was spayed parallel direction of sample placement from the top of the chamber and hence roughness played dominating role in ice accumulation.

It is important to select a coating material to meet specific application requirement to retain its properties for product life. Unless, though product may be promising at initial days of application, the durability and retention of icephobicity may be difficult to achieve.

The ice adhesion force of coated test panels were measured at frequent intervals during heat exposure (200^{o}C up to 60 days) and values are reported in figure 3.6. The unaged commercial superhydrophobic aerosol coating showed the lowest ice adhesion force of 15 KPa. However, after heat ageing for 60 days, the ice adhesion force increased to 55 KPa, which is similar ice adhesion value of heat aged silica-filled fluoro coating. Though silicone epoxy coating showed low initial ice adhesion, after heat exposure ice adhesion strength was increased to over 100 KPa.

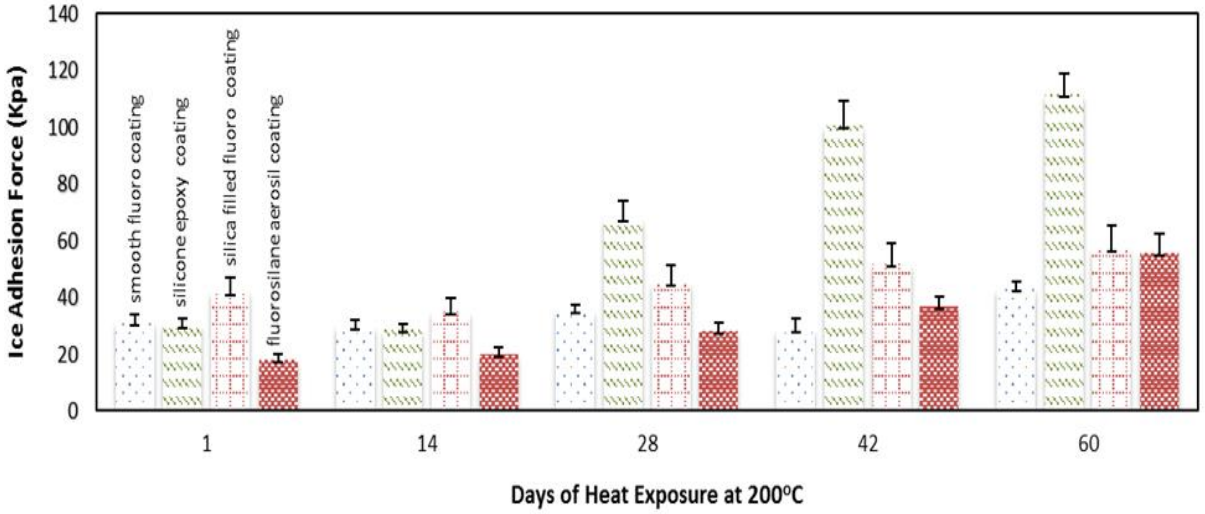

Figure 3.6. Ice adhesion force of the coatings tested at frequent intervals during heat ageing study at 200 ^{o}C.

The silicone epoxy coating and fluorosilane aerosol coating both had a change in surface roughness after heat exposure, with the implication of these change in surface roughness and texture pattern observed in the ice adhesion force as well [47-49]. The smooth fluoro coating did

not change much in surface roughness after heat exposure, and as expected, obtained the same observed ice removal force as well, which has maintained lowest among all other samples.

These ice adhesion strength values are ploted against work of adhesion using equation (1), the unaged coated panels data are reported in figure 3.7 (a) and aged coated panels values are reported in figure 3.7 (b). Unaged coated panels ice adhesion strength is linear with calculated work of adhesion, however aged samples data is not linear.

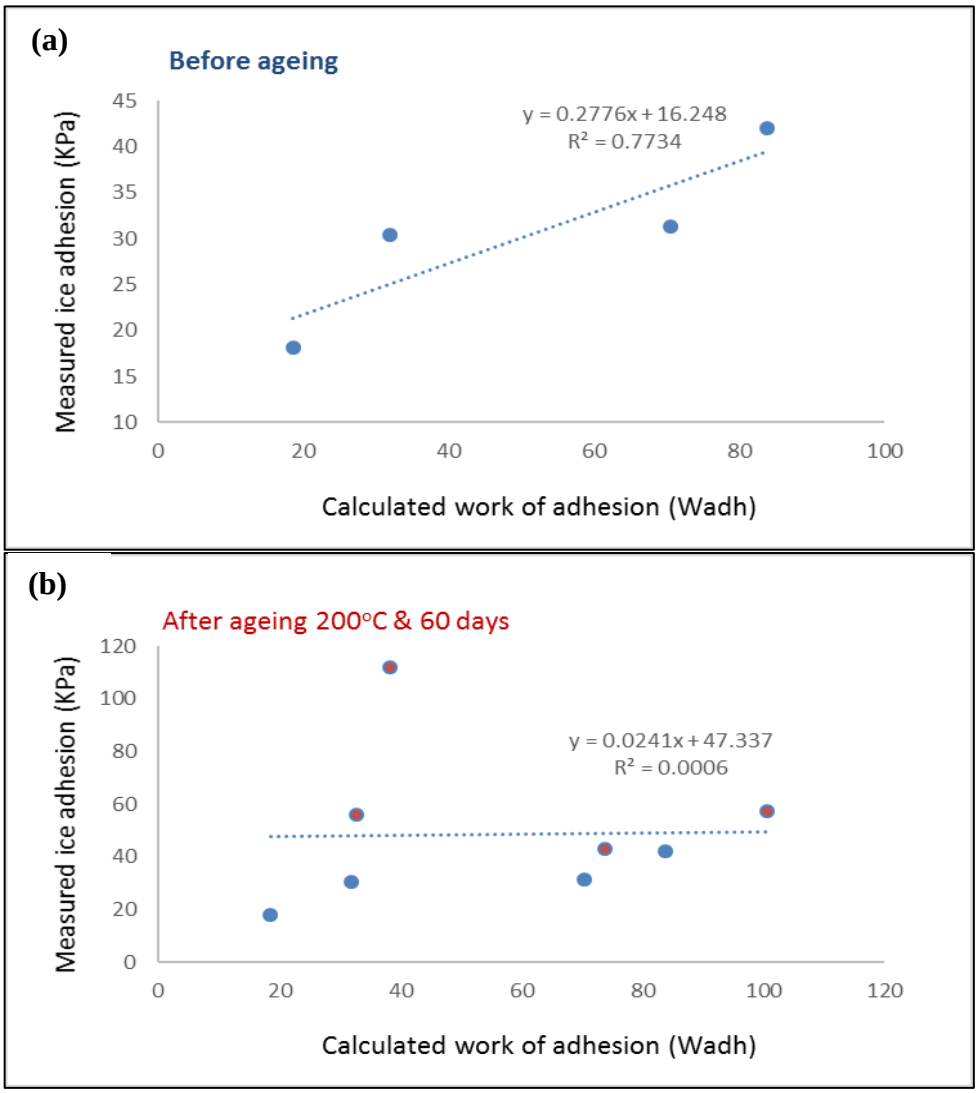

Figure 3.7. (a) Calculated work of adhesion of unaged coated panels, (b) Calculated work of adhesion of unaged and aged coated panels

Aged test panels work of adhesion strength was calculated using receding contact angle as same as unaged test panels. These results suggest that in addition to receding contact angle, other coating parameter may be influences the ice adhesion strength, which need to be evaluated further.

3.4 Summary and path forward

Water-based single layer FEVE smooth fluoro coatings and silica-filled fluoro coatings were prepared, tested and compared to commercially available silicone epoxy and a superhydrophobic fluorosilane aerosol coating. Vertical ice accumulation test data suggests that the smooth fluoro coating had less ice accumulation than the superhydrophobic fluorosilane aerosol coating. This result is in direct contradiction with most of the previous research reports [16,47 and 53], which report that higher contact angle provides better icephobicity and less ice accumulation. However, in this vertical (90^o) sample placement ice accumulation test, we did not observe the same. Hence, ice accumulation test method need to be automated and further robust to calculate rate of ice accumulation rather than only measuring ice weight initial and end of the test. Hence automated ice accumulation test method was developed for validation. Also, in addition to vertical sample placement, measuring ice accumulation with different same placement angles like 180^o, 45^o and 60^o could be valuable to understand influence of water wetting properties to ice accumulation as the water sliding angle of the coatings was significantly lower (ranges between 1^o to 10^o) than the ice accumulation test angle (90^o). Hence, the benefits of lesser water sliding angle and higher sliding angle may not have influenced these test results. Additionally, low ice adhesion force benefit was not observed in these coatings, hence a separate test is needed to quantify the practical application benefit of low ice adhesion force.

Though before heat aging commercial coatings has shown better icephobic performance, after high temperature heat ageing exposure to extend periods (60 days) the silicone epoxy coating and the fluorosilane aerosol coating were not able to retain their surface morphology and ice-phobic properties. However, the FEVE dispersion-based smooth fluoro coating and silica-filled fluoro coating showed excellent retention in icephobic properties after high temperature ageing exposure.

This research results, reconfirms the requirement of coating durability test for specific application requirements. Smooth fluoro coating needs to be studied with other durability test conditions like UV ageing, abrasion and water immersion to evaluate additional icephobic performance durability. These additional durability data can add value to explore commercial application feasibility of newly developed icephobic coatings.

4. UNDERSTANDING OF SILCIONE COATING ICE ADHESION PERFORMANCE

All lab-work in this chapter was performed by Sathish Kumar Ranganathan. All data analysis was performed by Sathish Kumar Ranganathan with guidance by Prof. Jeffrey P. Youngblood and John Howarter. All writing was performed by Sathish Kumar Ranganathan with guidance and editing by Prof. Jeffrey P. Youngblood and John Howarter.

4.1 Introduction

Ice buildup on structures and products can be hazardous, leading to human safety issues and economic challenges. Power transmission, aerospace, telecommunication, and transportation industries are the most affected by severe ice storms and ice accumulation [4,10,77 and 83]. To overcome these challenges resulted from ice accumulation on the product surfaces, several material development approaches and mechanisms have been explored. [84]. Elimination of accumulated ice from the surfaces achieved by reduction of ice adhesion force between ice and product surfaces. This force is measured as ice adhesion strength (KPa) of icephobic coatings to evaluate the ability of ice to fall away from the substrate or easy removal of ice from the substrates through external forces like wind, vibration, rotation, and other types of shear forces that are applied on the solid surface [76]. Extensive studies performed in this regard have proved that for producing surfaces with low ice adhesion strength, the coating materials should have the following characteristics: low surface energy, higher contact angle, reduced surface roughness, and less in elastic modulus to obtain surfaces with these properties, multiple methods and experimental approaches have been explored, primarily through altering material chemistry, surface lubrication and various coating approaches. These materials were further evaluated its influencing factors such as water wettability and material modulus to ice adhesion strength.

4.1.1 Role of water wettability to ice adhesion strength

The water wettability performance was explained by researchers using parameters like surface roughness, surface energy, water contact angle and hysteresis. Meuler et al. [54], have studied the role of water contact angle to the ice adhesion strength and observed that superhydrophobic surfaces can provide low ice adhesion strength. Like experimental observations, theoretical relationship also reported by Gao et al. [56] to correlate ice adhesion strength to water wetting properties.

4.1.2 Role of material modulus

Coating material modulus plays a critical role in anti-ice performance. Multiple research studies have been explored to validate its effect on ice adhesion strength. Zhuwei He et al. [43] analyzed the ice separation mechanism using low modulus silicone materials and explained macro scale crack mechanism on low modulus elastomers with rigid solid ice interface. In this work PDMS smooth surface, PDMS sponge and pillar shapes were used to demonstrate this mechanism. The experiments results suggest that combination of macro-crack and nano-crack could lead to super low ice adhesion strength [41-43]. Similarly, Beemer et al. [47] experimental results and Viswanathan et al. [88] theoretical work elaborated ice separation from the soft elastomer through "stick-slip dynamics and slow wave propagation". These experimental and theoretical broadly provides strategy to obtain an anti-ice surfaces using low modulus materials.

However, there is a practical limitation to utilize above mentioned materials and mechanisms for industrial applications. For example, superhydrophobic coatings could help to lower the ice adhesion strength; though having superhydrophobic surface is always preferred by product developers to achieve icephobic surface, developing superhydrophobic surface specific application and retaining its surface topography for product lifetime is highly difficult.

Considering material durability, application requirements, exterior environmental challenges, manufacturing requirements and cost, earlier mentioned recommendations and limitations need to be overcome by creating broader material design space to have flexibility to use coatings to achieve anti-ice surfaces. To identify and evaluate broader material design space, we considered silicone coating material, since it comes with advantage easy engineering feasibility of its properties. The silicone material selected with elastic moduli ranging from 8 psi to 280 psi selected to further tune its surface wetting properties (hydrophilic, hydrophobic, and superhydrophobic) and surface roughness values (3000 GS, 300 GS, and 30 GS) to measure ice adhesion performance.

4.2 Material and methods

4.2.1 Coating materials

To evaluate the ideal coating design space for achieving lower ice adhesion strength, silicone coating materials with different moduli were purchased from Smooth-On, Inc., sold under trade names Ecoflex, Dragon Skin, Equanex, and Smooth-sil. These silicone elastomers are prepolymers without a solvent (Part A and Part B), they were mixed in a specific mixing ratio and prepared as hydrophobic coatings. To prepare hydrophilic coating, silicone-glycol was added at 2.5 wt.% as the third component with the prepolymers. The silicone-glycol surfactant was purchased from AB Specialty Silicones, sold under the trade name Andisil SP-19, with a solid content of 98%. A superhydrophobic surface was as obtained by spraying a fluorosilane coating on the hydrophobic silicone surface. This superhydrophobic fluorosilane coating was procured from Water-Bead company, sold under the trade name Water-Bead and was supplied in pressurized metal container.

4.2.2 Preparation of the coatings and test panels

All the prepolymers were mixed in a 1:1 ratio except for Smooth-sil which was mixed in a 10:1 ratio. To prepare the coating material, Part B was added first and stirred for 5 minutes at 50 rpm using a lab coating mixer and then Par A of the same weight was added. Then the mixing was continued for 3 minutes before it was used to coat aluminum panels. To evaluate the ice adhesion strength and other properties, 5 "×5" aluminum test panels were used as substrates. The mixed coating material was applied on the aluminum panel using a sponge brush, followed by smoothening with a brass sheet to obtain a uniform coating surface. The coated panels were cured at ambient condition for overnight. To measure modulus and hardness of the coatings, the mixed silicone material was poured on the glass mold and cured for overnight. These cured rubber samples were about 45 mil thickness and it was cut to specific dimension before using for mechanical tests.

To prepare hydrophilic coatings, 2.5 wt.% of the silicone-glycol surfactant was added to the silicone coating mixtures and applied on the aluminum panels. These panels were cured overnight at ambient conditions for further testing. The superhydrophobic fluorosilane coating was sprayed on the pre-cured silicone-coated aluminum test panels, the distance between the panels and the container spray tip was maintained at approximately 10” to 12" to achieve a uniform surface finish. To prepare rough surfaces, sandpapers with different grit sizes such as 30, 300, and 3000 were used. After preparing the silicone coated test panels, the sand papers were placed on the coating surface to obtain sand paper roughness impression on the silicone surface. The silicone coating and along with sandpaper were cured overnight. After silicone material is cured, the sandpaper is removed, and test panels were used for further testing. Figures 4.1 and 4.2 shows the

schematics of the preparation steps to create different roughness and as well different contact angle.

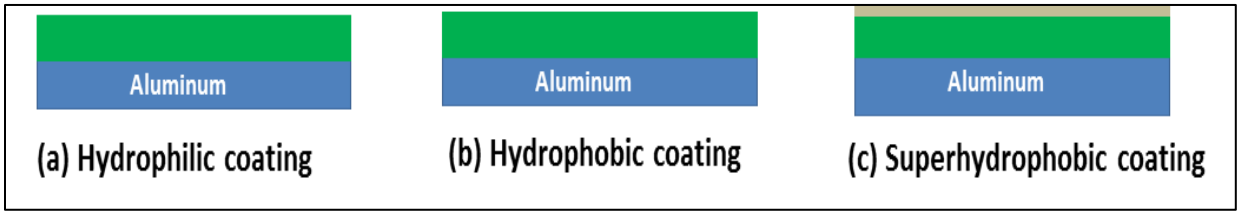

Figure 4.1. Illustration of smooth surface test panels

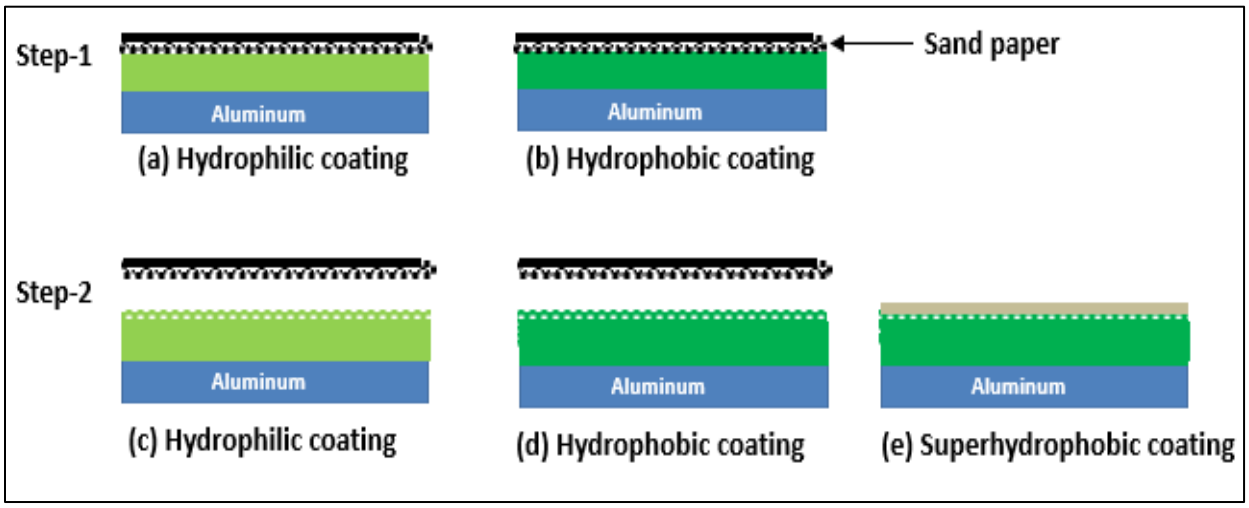

Figure 4.2. Illustration of rough surface test panels preparation steps

4.2.3 Analytical methods

Quantifying the ice adhesion strength of the coatings would help to understand easy removal of ice from the surface, by its own weight or by external forces such as wind or vibrations [76]. The ice adhesion of the silicone coatings test samples was prepared with range of elastic moduli, varying surface wettability and roughness. The surface wetting properties such as the advancing contact angle (ACA) and receding contact angle (RCA) were measured at room temperature. The water contact angle measurements were carried out using a 10 µl water droplet. The detailed measurement method was already discussed in previous chapter. The hardness of the silicone materials was measured using a hand-held shore A hardness meter; the indenter was

pressed on the rubber and the displayed hardness value was noted. The elastic moduli (E) of precut rubber samples (1 inch * 5 inch * 45 mil) were measured using a Zwick 1455 universal testing machine. The average values of three measurements were recorded as the elastic moduli of the various coating materials.

The surface characteristics of the coated aluminum test panels Ra and Rz roughness were analyzed to understand the influence of surface roughness on the ice-phobic performance. Ra roughness is calculated by averaging peaks and valleys of the roughness profile. Rz is calculated by measuring the highest peak to the lowest valley within a sampling area by averaging these distances. Rz averages only the five highest peaks and the five deepest valleys. Hence most Rz values are larger than Ra roughness values. The surface roughness was measured using Mahr PS1 digital contact profile meter with "v" sharp profile tip. The surface contact probe diameter of 2 µm and length 1mm were used to measure smooth and 3000 GS surface roughness, the probe diameter of 5 µm and length of 1mm were used to measure 300GS surface roughness and the probe diameter of 5 µm and length of 8mm were used to measure 30GS surface roughness. The surface roughness measurable ranges are from 0.1 to 500 µm. Roughness was measured at four different locations of the same test panel and average value is reported.

The coating surface image was taken using A Dino-lite digital microscope and reported as qualitative comparison between different roughness scale. The ice adhesion force was measured by applying shear stress to the cylindrical ice block adhered to a coated test panel. To form the ice block on the coated test panel, a water-filled cylindrical container was kept on the coated panel at -10 ^{o}C for 24 hours. The container had an inner diameter and a height of 3". After cylindrical ice block was formed on the coated test panel, it was fixed to a Zwick 1455 universal testing machine

to perform the adhesion force test. The ice adhesion test was conducted inside a cold chamber maintained at -10^{o}C and at least five trials were performed to obtain the average ice adhesion force.

4.3 Result and discussion

The mixed silicone materials are hydrophobic by design as it is purchased. The silicone material after mixing and curing it shows hydrophobic nature. Other properties like modulus and hardness were measured and reported in table 4.1 below. The silicone coating material modulus range was varied from extreme low of 7.8 psi to high of 282 psi. The same material shore A hardness were ranged from 1 to 60. These materials appropriately selected for further surface properties like contact angles and roughness modification and were further validated against ice adhesion strength to understand influencing role of the same.

Table 4.1. Properties of silicone materials

Sample name	Coatings	Modulus, E (psi)	Hardness (shore-A)	ACA (^{o})	RCA (^{o})	CAH (^{o})
S1	Eco-flex 00-10	7.8 ± 1.2	1.0 ± 0.1	104.2 ± 1.8	82.1 ± 1.2	22.1
S2	Eco-flex 00-50	13.6 ± 3.6	5.0 ± 0.4	104.8 ± 1.2	82.0 ± 1.8	22.8
S3	Dragon Skin 10	23.0 ± 4.1	10.0 ± 0.5	105.1 ± 3.7	82.1 ± 2.2	23
S4	Dragon Skin (10+30)	54.1 ± 5.0	22.3 ± 0.8	105.3 ± 2.1	82.3 ± 2.8	23
S5	Dragon Skin 30	88.0 ± 4.8	30.0 ± 0.8	105.8 ± 2.1	82.4 ± 1.9	23.4
S6	Equanex 40	121.4 ± 6.5	40.1 ± 1.1	105.8 ± 1.9	82.6 ± 2.7	23.2
S7	Equanex 40 + smoothsil 950	189.1 ± 9.2	45.5 ± 2.0	106.1 ± 1.7	82.7 ± 2.1	23.4
S8	Smoothsil 950	264.7 ± 19.2	50.0 ± 1.7	106.2 ± 3.2	83.8 ± 1.9	22.4
S9	Smoothsil 960	282.0 ± 15.0	60.2 ± 1.8	106.2 ± 2.1	84.1 ± 1.8	22.1

4.3.1 Role of coating modulus and surface energy in determining ice adhesion strength

The surface energy of the silicone coating was referred from previous studies [85-86] and the average value of 23mN/m is considered here to plotting graph with combination of surface energy and elastic modulus and against ice adhesion strength in the figure 4.3. As combined product of modulus and surface energy increases, the ice adhesion strength also increases. The lowest ice adhesion strength was observed between coating modulus 10 psi to 25 psi. The combination of surface energy and modulus to ice adhesion strength plot follows similar trend of adhesion theory explained by Baier [60] and the calculated linear plot R^2 value is 0.88. These results provide valuable information of ice adhesion strength relation to modulus for smooth hydrophobic material.

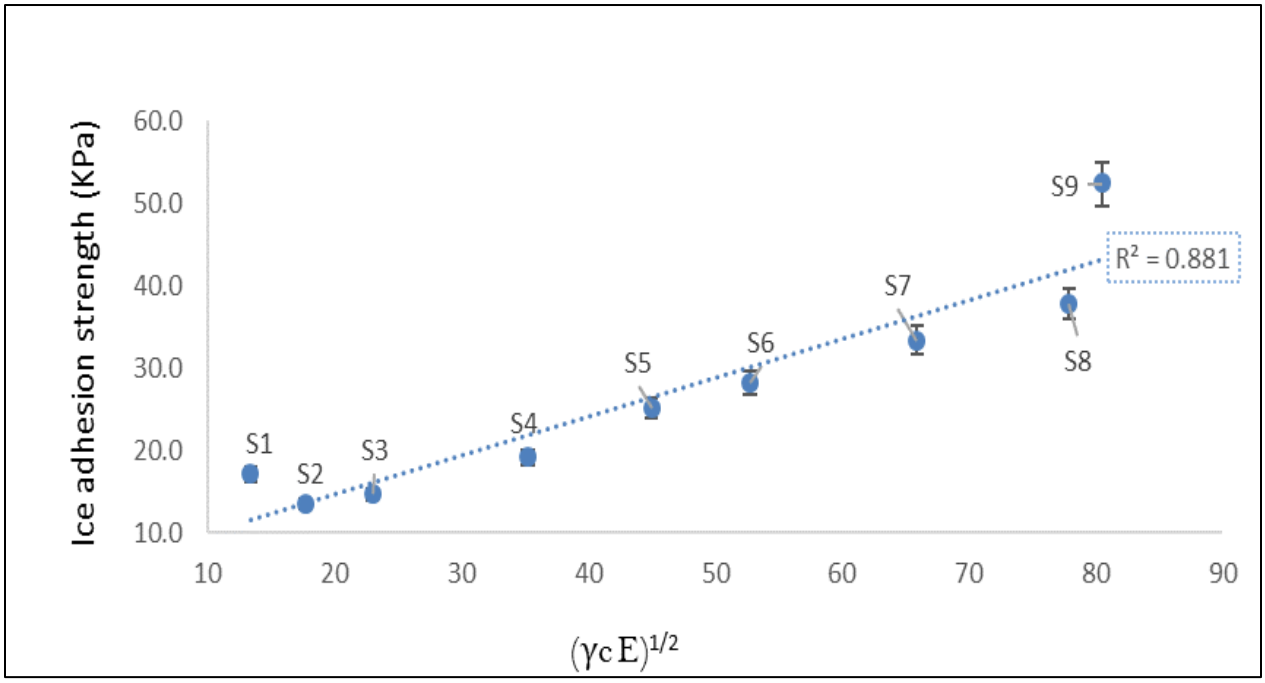

Figure 4.3. Combination influence of coating modulus and surface energy to ice adhesion strength

4.3.2 Influence of roughness on ice adhesion strength

To evaluate the influence of coating roughness to ice adhesion strength, silicone coatings (S3, S5, S6, and S7) with varying elastic modulus ranging from 23 psi to 282 psi were selected. The coating surface roughness was modified by using sandpaper impression during coating curing process as described earlier. The digital images of the sandpaper with different grain sizes (3000, 300 and 30 grain size) and coating surfaces with roughness are reported in figure 4.4. The image shows different surface roughness of the coating with varying grit sizes, surface roughness produced using 30 GS sand papers is high as compare with silicone surface prepared using 300 GS and 3000 GS. Surface roughness Ra and Rz was measured using contact profile meter. The roughness data is reported in table 4.2. The high modulus coating (S9) seems to have relatively less Ra roughness as compare to coatings S7 and S5. The primary reason is the S9 material with high modulus and hardness has resistance to form sand paper impression on the surface. The Rz roughness of 30 grit size sandpaper made coatings was above the instrument measurable higher limit (500 µm), hence the Rz roughness value is reported as >500 µm

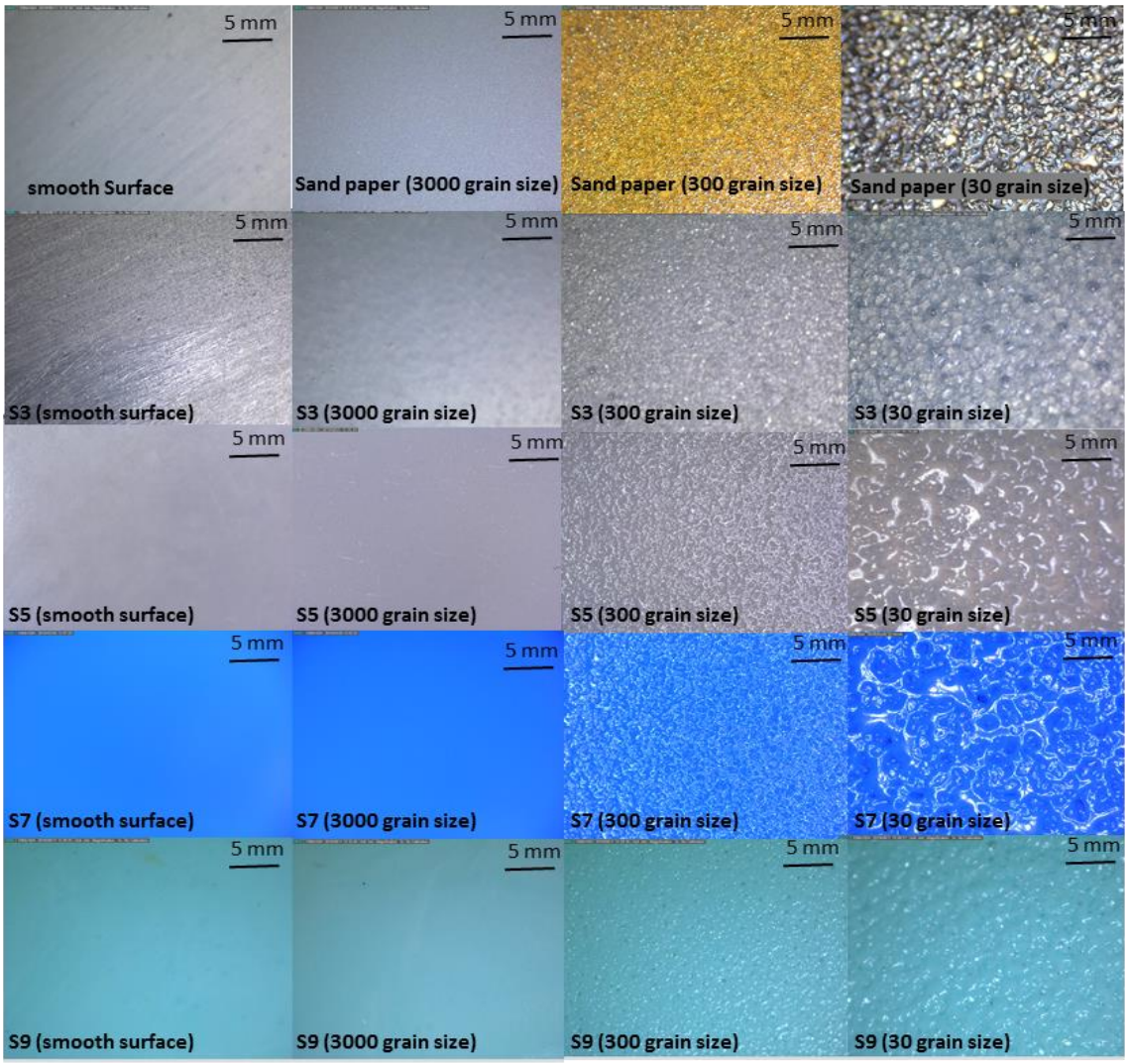

Figure 4.4. Optical images of sand paper and silicone samples

Table 4.2. Silicone coated test panel surface roughness

Coated samples	Ra, roughness, microns				Rz, roughness, microns			
	Smooth	3000 GS	300 GS	30 GS	Smooth	3000 GS	300 GS	30 GS
S3	0.6 ± 0.1	2.9 ± 0.3	14.5 ± 3.0	326 ± 32	3.5 ± 0.5	19.5 ± 2.8	42.5 ± 11	> 500*
S5	0.7 ± 0.1	3.1 ± 0.4	18.4 ± 4.5	365 ± 48	3.4 ± 0.3	24.0 ± 3.4	77.1 ± 16	>500*
S7	0.8 ± 0.1	3.2 ± 0.4	19.5 ± 4.1	388 ± 70	3.2 ± 0.3	27.5 ± 5.1	96.5 ± 18	>500*
S9	1.0 ± 0.2	3.2 ± 0.7	16.8 ± 3.8	355 ± 55	3.2 ± 0.4	26.2 ± 4.4	64.0 ± 12	>500*

To understand the role of coatings surface topography to ice adhesion strength, hydrophobic silicone coating smooth and rough surfaces using 3000 GS, 300 GS and 30 GS sandpapers were prepared. The ice adhesion strength test results are plotted in figure 4.5. Smooth surface ice adhesion strength was changed moderately (ranges from 15 psi to 60 psi) while increasing the elastic modulus of silicone materials from 23 psi to 282 psi. Though the modulus scale is increased ten folds, ice adhesion strength is not increased significantly. The possible ice removal mechanism can be explained using previous research work [87-90], since silicone surface is hydrophobic and during ice adhesion test, once ice crack initiated at the edge of the sample, it can rapidly have detached from entire ice from the silicone surface. Though smooth surfaces provide low ice adhesion strength, during exterior application usage, the product surfaces are being exposed to external pollutants, which are prone to effect coating surface smoothness with the damage created by exterior sand, dust and pollution over the course of time [1,47, 91 and 92]. Hence, considering those application scenarios, we introduced the roughness on the coating surface from minor scale 3000 grit size to large scale roughness of 30 grit size and have studied influence ice adhesion strength to roughness.

Surprisingly, ice adhesion strength of low modulus materials (23 psi and 88 psi) rough surface did not change significantly, even with increasing Ra roughness from 3.2 µm to 355 µm. This observation is contrast with Zou [57] and Markus Susoff [46] findings, wherein they have reported that increase in surface roughness increases the ice adhesion strength by mechanical interlocking due to the increased surface contact area between ice and coating at the interface. However, low modulus material tolerance to roughness possibly explained by two different mechanisms which was demonstrated by researchers. Z. He and others [49, 81 and 88] reported that when shear force applied on soft elastomers using rigid ice, the macro crack is initiated at the

interface, which can lead to significantly low ice adhesion strength. Similarly, Viswanathan [90] elaborated “stick-slip dynamics and slow wave propagation”, whereas macro crack initiation and propagation is overruling the mechanical interlocking which is expected at the ice and polymer interface.

Above mentioned macro crack and slow wave propagation mechanisms for low modulus or soft elastomers makes more compellable, as we compare ice adhesion strength of higher modulus materials (189 and 282 psi). Since, the ice adhesion strength of higher modulus materials rough surface was increased significantly as compare to smooth hydrophobic silicone coatings. These increase in ice adhesion strength was observed even with minor introduction of Ra roughness (3.2 µm). As compare to smooth surface, the ice adhesion strength of rough surfaces was increased from 49 KPa to 155 KPa for 189 psi material and 63 KPa to 168 KPa for 282 psi material. If we compare ice adhesion strength of lowest modulus material (23 psi) to highest modulus material (282 psi) rough surfaces, the ice adhesion strength increased from 20 KPa to 168 KPa, this result was almost linear trend with increase of material modulus to ice adhesion strength. The same kind of linear increase were not observed for smooth surfaces. Interestingly, further increase of Ra roughness from 3 µm to 350 µm did not aggravate much ice adhesion. The increase ice adhesion strength with roughness was much explained by previous researchers by various mechanisms and most common mechanism is mechanical interlocking of rigid coating surface and the solid ice at the interface during ice formation [16 and 46] Hence, from our experimental results,

it can be derived that up to a critical material modulus of about 100 psi, the surface roughness was not significantly influencing ice adhesion strength.

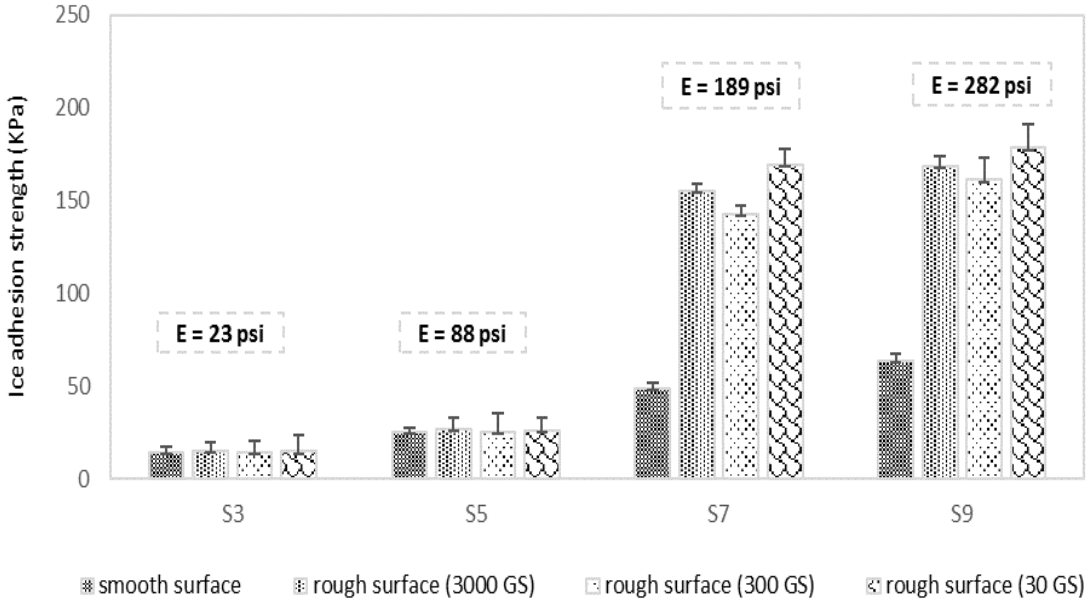

Figure 4.5. Ice adhesion strength of low to high modulus (S3, S5, S7, and S9 respectively) silicone coatings with smooth and rough surfaces; Elastic modulus (E) values are mentioned inside the graph

Additionally, the failure created at higher modulus rough surfaces is due to the micro crack initiated at the ice [87-90]. To validate this, after the ice adhesion test, surface images of the ice were taken and reported in figure 4.6.

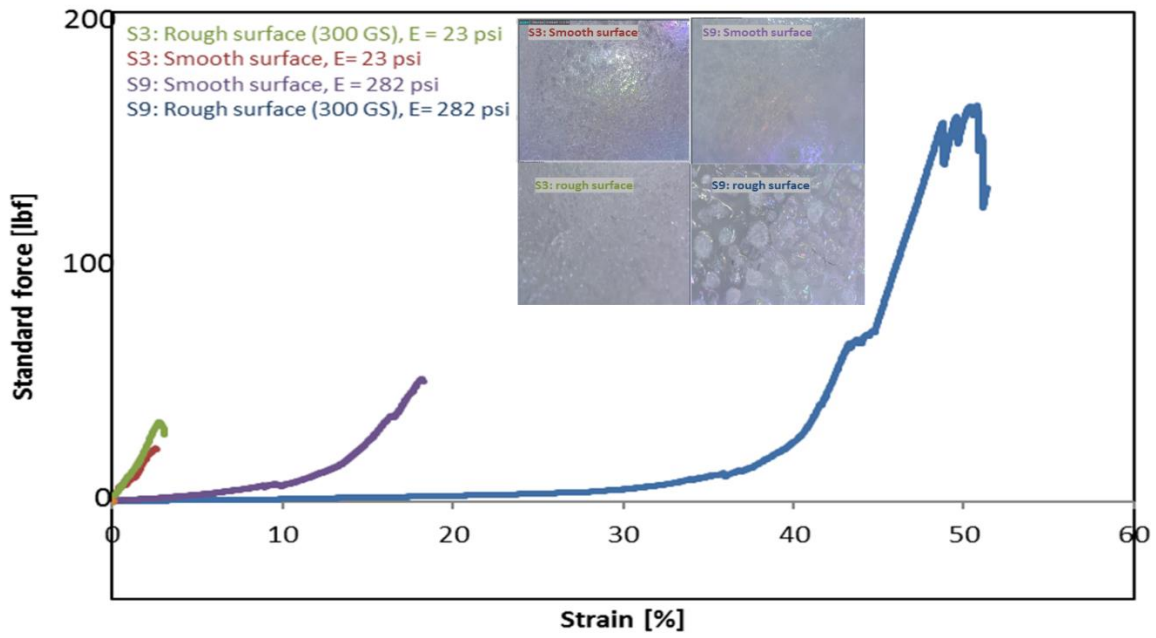

Figure 4.6. Ice adhesion test stress – strain curve and images of the ice after the test

The ice adhesion stress-strain curve suggests that rough surfaces yield at higher (higher force?) as compare to smooth surfaces. The ice images of low modulus (S3) smooth and rough material did not show any cracks at the surface, however the higher modulus material (S9) rough surface ice images show cracks on the ice surface. This observation aligns with Z. He et. al. and Viswanathan et. al [87-90] research work which reported that low modulus material surface ice separation happens by stick-slip mechanism. However higher modulus material ice separation was happened due the crack-initiated fracture on the ice, which explained by following equation [5] $\tau = \sqrt{\frac{E\,Grec}{\pi a}}$ explained by Nosonovsky et. al. [2], wherein E is ice modulus (9.7 GPa), "a" is crack length which influences the fracture and G is surface energy of the crack which is calculated using receding water contact angle, and same as work of adhesion calculated using equation (3).

These insights can help to create a much-needed anti-ice design space, wherein the coating material critical modulus and roughness plays an influencing role. Having said that anti-ice

material design space would not be complete and justifiable unless evaluating with water wetting property. Hence, we further analyzed the role of water contact angles to the ice adhesion strength.

4.3.3 Effect of surface wetting properties on ice adhesion strength

The role of surface wetting properties to ice adhesion strength was analyzed using hydrophilic, hydrophobic and superhydrophobic coatings. These coatings were prepared as smooth and as well as rough surface. The rough surface was prepared using 300 grit size sand paper. The measured water contact angles of coatings are reported in table 4.3. The hydrophilic coating smooth and rough surfaces advance contact angle (ACA) were observed between 71^o to 79^o and receding contact angle (RCA) were between 47^o to 52^o. The hydrophobic coating smooth and rough surfaces ACA were measured between 105^o to 114^o and RCA were ranged between 82^o to 91^o. The superhydrophobic coating smooth and rough surfaces, ACA was between 152^o to 158^o and RCA ranged between 138^o to 147^o. Superhydrophobic coatings contact angle hysteresis (CAH) are among lowest as compare to hydrophobic and hydrophilic coatings. Comparatively between smooth and rough surfaces, the slight increase in contact angle were observed due to potential reduction is contact area or through air pockets [22]. The influence of water contact angle to ice adhesion strength were further validated and reported as smooth and rough coating ice adhesion strengths in figure 6a and 6b respectively.

Table 4.3. Contact angle values of hydrophilic, hydrophobic, and superhydrophobic smooth and rough surfaces

Coating type	Hydrophilic						Hydrophobic						Superhydrophobic					
Surface type	Smooth surface			Rough surface (300GS)			Smooth surface			Rough surface (300GS)			Smooth surface			Rough surface (300GS)		
Sample name	ACA (^{0})	RCA (^{0})	CAH (^{0})	ACA (^{0})	RCA (^{0})	CAH (^{0})	ACA (^{0})	RCA (^{0})	CAH (^{0})	ACA(^{0})	RCA (^{0})	CAH (^{0})	ACA (^{0})	RCA (^{0})	CAH (^{0})	ACA(^{0})	RCA (^{0})	CAH (^{0})
S3	71.2 ± 1.3	47.6 ± 1.8	23.6	72.6 ± 2.1	47.7 ± 0.4	24.9	105.1 ± 3.7	82.1 ± 3.2	23	106.1 ± 4.2	87.3 ± 3.2	18.8	152.1 ± 2.4	138.1 ± 3.2	14	155.1 ± 2.1	144.3 ± 2.8	10.8
S5	72.4 ± 2.1	48.5 ± 2.1	23.9	72.1 ± 1.8	49.1 ± 0.6	23	105.8 ± 2.1	82.4 ± 1.9	23.4	107.9 ± 7.1	88.0± 2.0	19.9	153.7 ± 3.1	139.0 ± 4.9	14.7	156.2 ± 1.8	144.5 ± 3.2	11.7
S7	74.1 ± 1.0	49.2 ± 3.2	24.9	77.0 ± 2.6	51.2 ± 1.2	25.8	106.1 ± 1.7	83.1 ± 2.1	23	112.1 ± 4.1	88.4 ± 6.1	23.7	153.2 ± 2.1	140.2 ± 3.4	13	157.1 ± 3.2	145.2 ± 4.8	11.9
S9	75.9 ± 2.5	49.6 ± 4.2	26.3	78.3 ± 1.4	51.1 ± 2.1	27.2	106.2 ± 2.1	82.6 ± 1.8	23.6	114.6± 3.2	90.7 ± 4.2	23.9	154.6 ± 1.8	142.2 ± 2.7	12.4	158.5 ± 4.1	146.2 ± 3.8	12.3

The ice adhesion strength of smooth surfaces results (figure 4.7 a) suggest that, hydrophilic coating has higher ice adhesion strength than the hydrophobic and superhydrophobic coatings for the test material modulus. Hydrophilic and hydrophobic coatings, ice adhesion strength was increased as the coating modulus increases. Hydrophilic coating ice adhesion strength was 18 KPa for 22 psi modulus coating, whereas for high modulus coating (280 psi), the ice adhesion strength was tripled to 60 KPa. Similarly, hydrophobic coating ice adhesion strength was more than doubled from 20 KPa to 50 KPa. However, ice adhesion strength superhydrophobic coating was not increased significantly with the increase in modulus. Superhydrophobic coating ice adhesion strength was lower than 30 KPa for all the modulus materials. Hydrophilic and hydrophobic coatings ice adhesion strength values were increased with the rise of material modulus, which follows similar to adhesion theory explained by Baier [60]. The calculated linear regression plot R^2 value for hydrophilic and hydrophobic coatings are 0.98 and 0.96 respectively. However, superhydrophobic coatings the rate of increase is nor rapid as like other coatings, its linear regression plot R^2 value is 0.76.

Ice adhesion strength of rough (figure 4.7 b) hydrophilic and hydrophobic surfaces both has resulted in moderate increase ice adhesion strength for lower modulus coatings (23 psi and 88 psi), however at higher modulus coatings (189 psi and 282 psi) the increase in ice adhesion strength

were seen multifold. Hydrophilic coating ice adhesion strength increased from 20 KPa to 190 KPa with increase in material modulus from 23 psi to 282 psi. Similarly, Hydrophobic coating ice adhesion strength were increased from 18 KPa to 160 KPa with increase in material modulus from 23 psi to 282 psi. Interestingly, superhydrophobic coating has retained its low ice adhesion strength performance across all the material modulus level. The maximum observed ice adhesion strength was 32 KPa for 282 psi material modulus. It is important to note that superhydrophobic coating had highest receding angle and lowest contact angle hysteresis (CAH).

These test results findings are similar to Meuler et al. [54] and Oberli et al. [55] experimental findings, whereas they have reported that receding contact angle and contact angle hysteresis plays a critical role in ice adhesion strength and both have recommended higher water contact angle, superhydrophobic surface to obtain low ice adhesion surfaces. Additionally, Z. He et al. [49] detailed the mechanism of nano-crack initiation of low surface energy and superhydrophobic surfaces. These mechanisms validate our test results and observations.

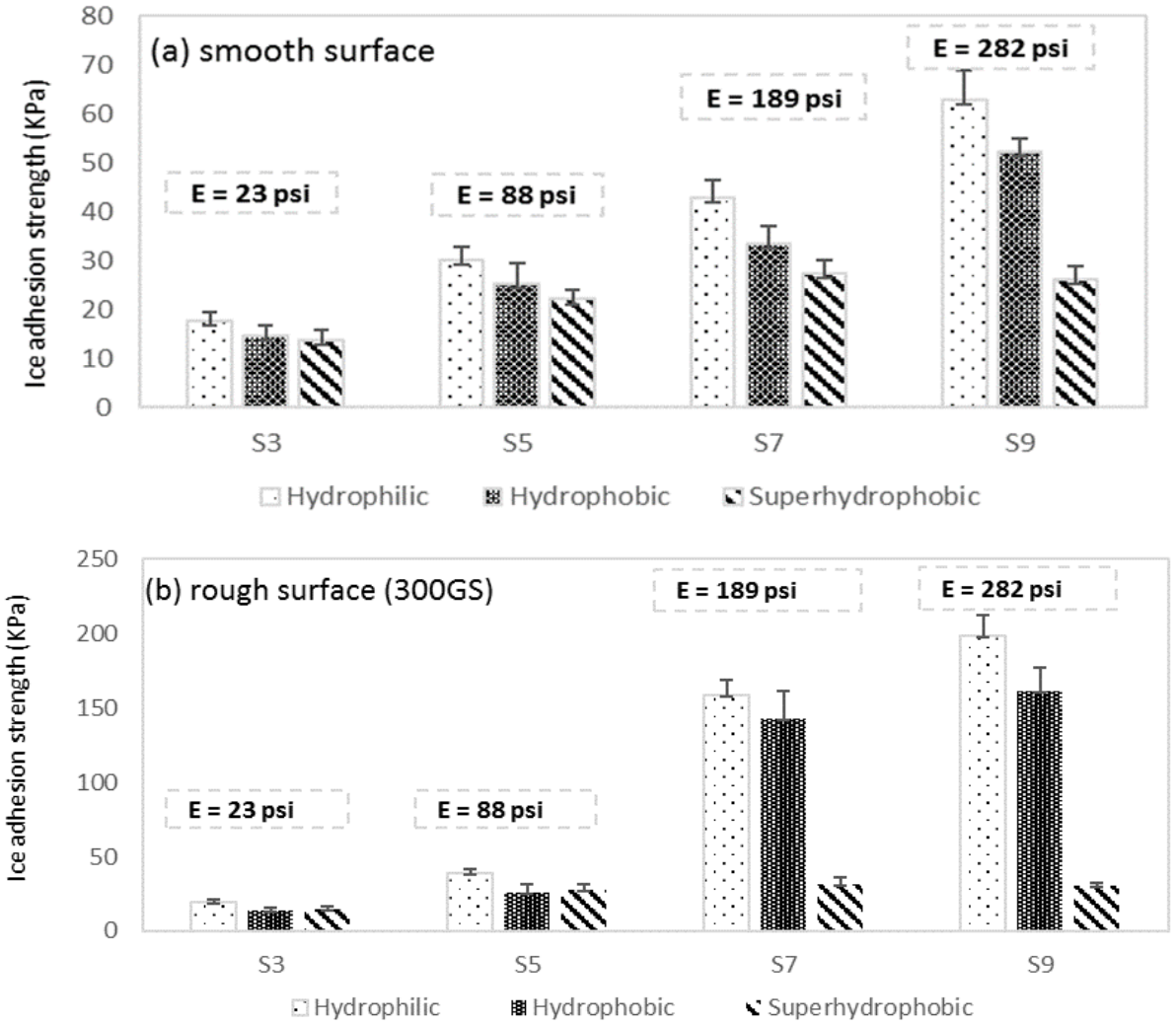

Figure 4.7. (a) Ice adhesion strength of smooth hydrophilic, hydrophobic and superhydrophobic surfaces, (b). Ice adhesion strength of rough hydrophilic, hydrophobic and superhydrophobic surfaces

Ice adhesion strength of smooth and rough surfaces were further evaluated with Baier's relationship [equation-4] and those plots are reported in figure 4.8 (a) and 4.8 (b). The smooth coating surface which performs like Baier's recommendation [60], which suggested that the adhesion strength is linear with combination of material modulus and surface energy.

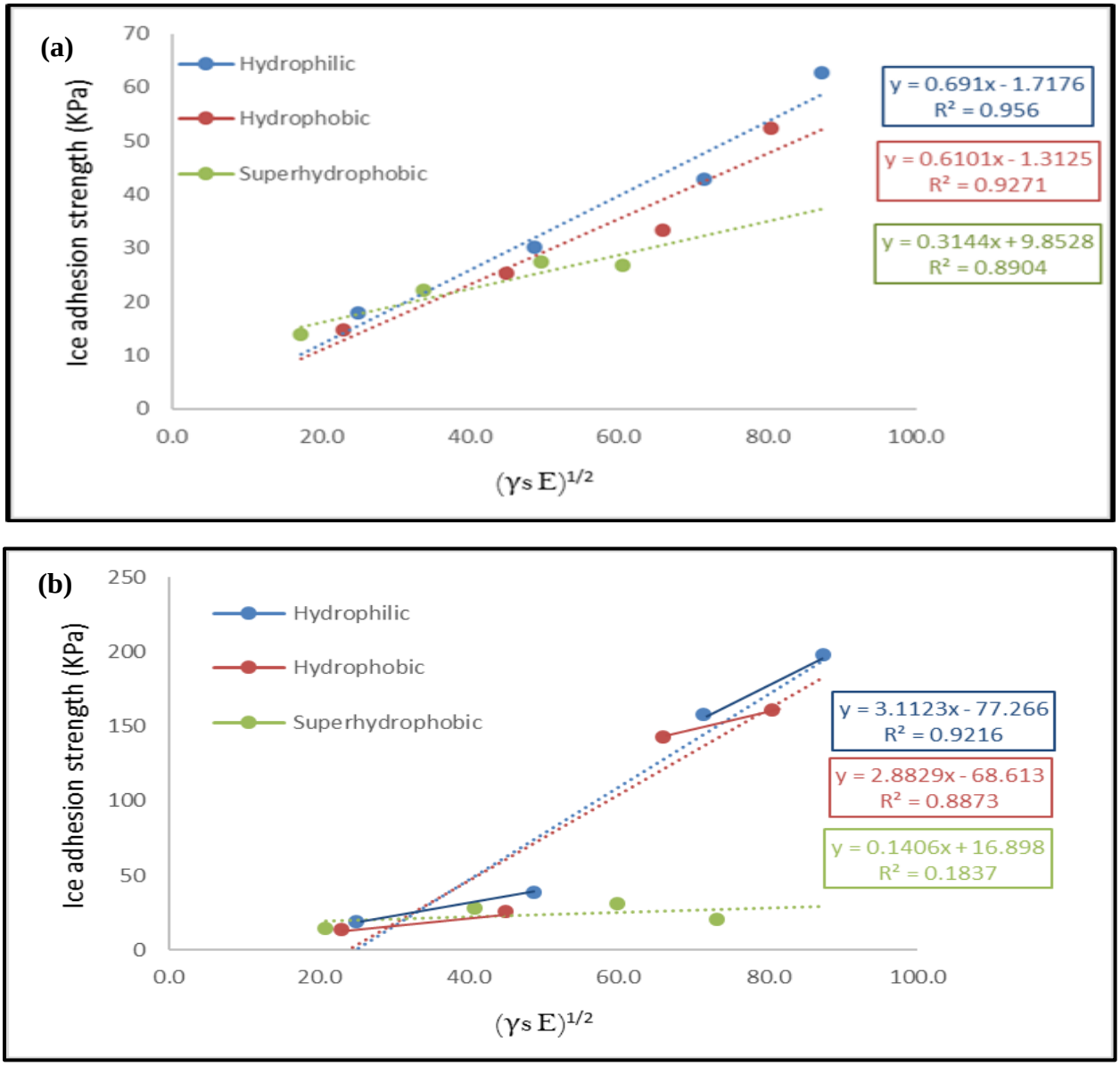

Figure 4.8. (a). Baier's adhesion plot for smooth surfaces, (b). Baier's adhesion plot for rough surfaces

However, rough surfaces ice adhesion strength plot suggest that hydrophilic and hydrophobic coating surfaces were not following linear relationship, especially between high modulus and low modulus coatings. This change in ice adhesion strength is primarily due to difference in modulus dependent crack initiation suggested by other researchers [87, 90]. Baier recommendation could have worked well, if material adhesion were not significantly

affected modulus or cracks were not influenced the adhesion results. However, superhydrophobic coating had showed a linear relationship with adhesion values across the material modulus, since superhydropbic ice adhesion strength did not influenced by change in modulus, due to its low surface energy and better icephobic performance achieved by nano-crack mechanism [87] which helps to obtain low ice adhesion strength. As we discussed earlier, the failure of ice break was not happened at the tensile strength yield, rather than failure was posted by fracture before it yields. It might be helpful, if adhesion strength relationship would be developed using combination of material modulus, surface energy and fracture energy.

Having said that, these observations eludes that superhydrophobic coatings are superior in anti-ice performance, it is not commercially feasible to obtain and use superhydrophobic coatings for all the applications, also even more difficult retaining of superhydrophobic surface for longer duration at exterior environment. Hence, for a specific application, selection of superhydrophobic coatings need to consider carefully reviewing other durability requirements. From figure 6b, it can be concluded that hydrophobic material also can provide low ice adhesion below critical modulus range (~ 100 psi). Hence, based on application requirements, material availability with reasonable cost and manufacturability, coatings can be selected, when earlier observed modulus and roughness conditions are met.

4.4 Summary and path forward

An attempt to create an anti-ice material design space with a reasonable material selection recommendation to product developers, considering industrial scale manufacturing and exterior application durability requirements, following conclusions were made.

1. Coating material modulus plays an influencing role to ice adhesion strength, along with surface roughness and water contact angle.
2. Surface roughness influences the ice adhesion strength above critical modulus (~100 psi).
3. Superhydrophobic coatings observed to be low in ice adhesion strength at all the modulus range
4. When hydrophobic coating is considered for anti-ice application, the coating material modulus need be less that critical modulus of 100 psi.

Based on above test results and observations, low ice adhesion strength surface can be obtained by using different influencing parameters such as contact angle, roughness and mechanical properties. The applications which has the constraints in terms of the substrate stiffness and roughness, such as power transmission lines superhydrophobic coatings could be considered [18-23]. For the applications such as roofing with no restrictions in terms of the coating modulus or roughness, either low-modulus coatings or superhydrophobic coatings can be chosen [47,62, and 71] For the applications, which has no limitations on thickness, roughness or coating properties, superhydrophobic surfaces with low elastic moduli materials could be considered to obtain an extremely low ice adhesion surfaces. Figure 4.9. shows the schematic representation of material design space to ice achieve low ice adhesion.

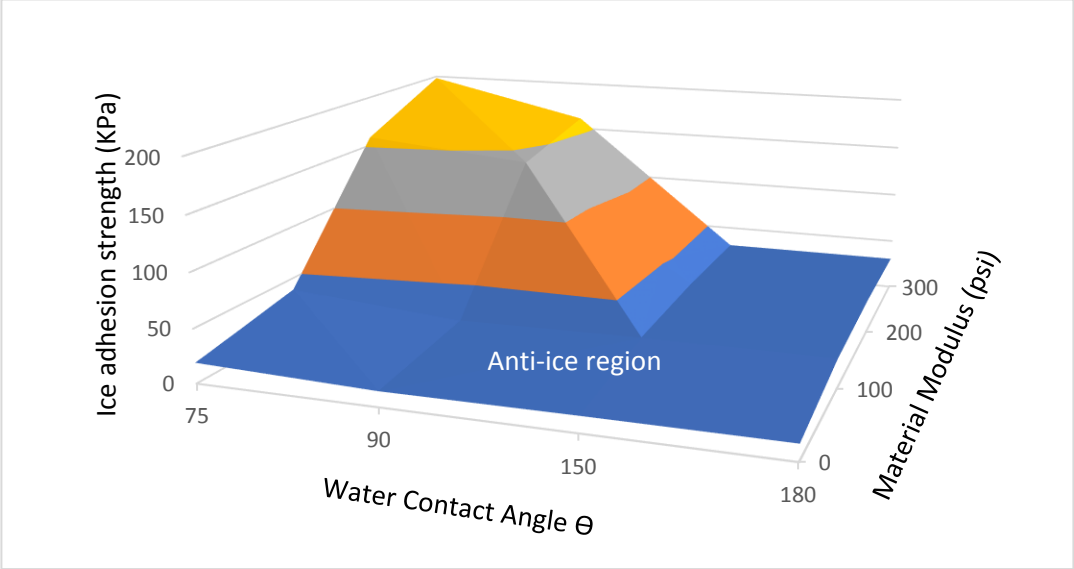

Figure 4.9. Schematic representation of material design space to ice achieve low ice adhesion

5. ICE ACCUMULTION TEST METHOD AND PERFORMANCE OF SILICONE COATINGS

5.1 Introduction

Early stage of ice formation and ice accumulation on the product surface can be evaluated by ice accumulation test method. Ice accumulation and ice weight build-up can increase the load of the products and structures [11, 38 and 48]. After ice is accumulated up to certain weight, the ice removal or ice weight reduction is resulted for some products. This ice removal or ice elimination can happen at two locations: 1) at the interface of product surface and ice, when the ice load is higher than the ice adhesion strength. 2) on the ice body itself, potentially due to ice cracks, as a response of weak ice strength to hold further ice build-up or combination effect of ice weight, cracks and due to the external forces, such as wind and vibration [3, 38 and 42]

To eliminate ice from the product surface and ice interface, low ice adhesion strength coating is preferred and to reduce amount of ice accumulation on the product or delay of early stage icing process, product surface with delayed or reduced ice nucleation and accretion is preferred [3, 42, 44 and 96]. To understand ice accumulation performance, coated test panels of low modulus (S3) and high modulus (S9) silicone coatings were prepared. Also, silicone coatings with different water contact angles such as hydrophilic, hydrophobic and superhydrophobic ranges were evaluated.

5.2 Ice accumulation results discussion

Ice accumulation test was performed at -10 ^{o}C, using automated ice accumulation test set-up (refer figure 2.3), the test panels were placed at the 60^{o} angle against water spray direction. The measured ice weight results are reported and discussed in following sessions.

5.2.1 Hydrophilic coating ice accumulation performance

Low modulus (S3) and high modulus (S9) hydrophilic silicone coatings, ice accumulation results were compared with smooth aluminum and sandblasted aluminum test panels. The ice weight increase test results are reported in the figure 5.1. Uncoated aluminum sheet had accumulated less ice as compare to sandblasted aluminum and hydrophilic silicone coated test panels. At the early stage ice accumulation process (between 256 to 1021 seconds) low modulus (S3) hydrophilic coating ice accretion rate slightly higher than sandblasted aluminum test panel.

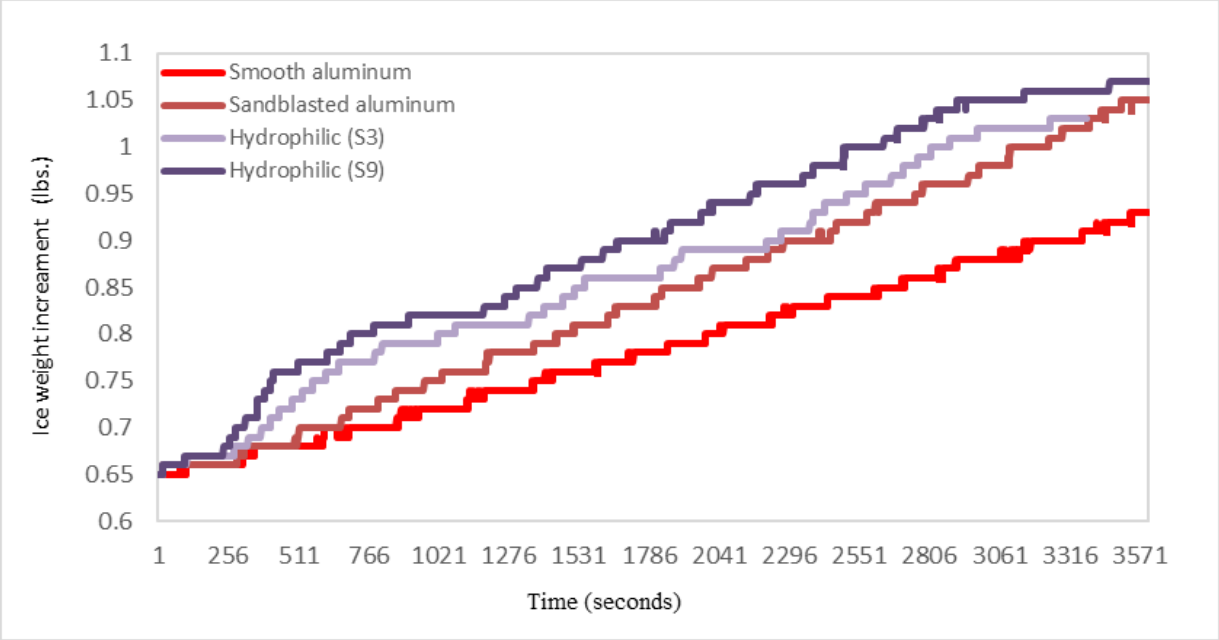

Figure 5.1. Ice accumulation weight increase of hydrophilic coatings

At the end of the test (after 3000 seconds) both samples have accumulated similar ice weight. The high modulus (S9) hydrophilic coating ice accumulation was slightly higher than low modulus (S3) coating and sandblasted aluminum surface. Important to note that advance contact angle of hydrophilic coatings (S3: 71.2 ± 1.3 and S9: 75.9 ± 2.5) and sandblasted aluminum (78.1 ± 4.2) were almost similar. Smooth aluminum advance contact angle (63.7 ± 2.2) is lesser than

hydrophilic coatings and sandblasted aluminum sheet. It was anticipated that low water contact angle test surface could lead to higher ice accumulation [3, 42 and 96]. However, the test results suggest that though smooth aluminum surface had a lowest water contact angle compare to other surfaces (sandblasted aluminum and hydrophilic coatings), it had accumulated less ice weight. The primary reason for this surprising result were that rough surfaces can have increased ice accumulation as compare to smooth surfaces [4, 42, 98 and 99]. The smooth aluminum sheet had lowest surface roughness (roughness, Ra: 0.8 µm ± 0.1 and roughness, Rz: 1.4 µm ± 0.2) as compare to sandblasted aluminum (roughness, Ra: 19.4 µm ± 2.4 and roughness, Rz: 58.4 µm ± 4.7 µm), low modulus hydrophilic silicone coating (roughness, Ra: 0.6 µm ± 0.1 and roughness, Rz: 3.5 µm ± 0.5) and high modulus hydrophilic silicone coatings (roughness, Ra: 1.4 µm ± 0.2 and roughness, Rz: 3.6 µm ± 0.3)

5.2.2 Hydrophobic coating ice accumulation performance

Low modulus (S3) and high modulus (S9) hydrophobic silicone coatings ice accumulation test was performed along with smooth aluminum and sandblasted aluminum surfaces. The ice weight increase test results are reported in figure 5.2. The ice weight increase of smooth aluminum and low modulus hydrophobic surface shows almost similar in ice weight increase, only with minor difference observed at the end of the test. Though the smooth aluminum expected to perform better in ice accumulation than the hydrophobic coating, due to its low roughness surface, both hydrophobic and smooth aluminum had similar ice weight increase. The primary reason is the water contact angle of hydrophobic coating (105.1 ± 3.7) is much higher than smooth aluminum (63.7 ± 2.2), that had contributed less ice accumulation [3, 43 and 67]. High modulus silicone coating (S9) and sandblasted aluminum surface had accumulated more ice as compare to

earlier mentioned test panels. These results observations are different from hydrophilic coated test panels, wherein smooth aluminum had a lowest ice accumulation.

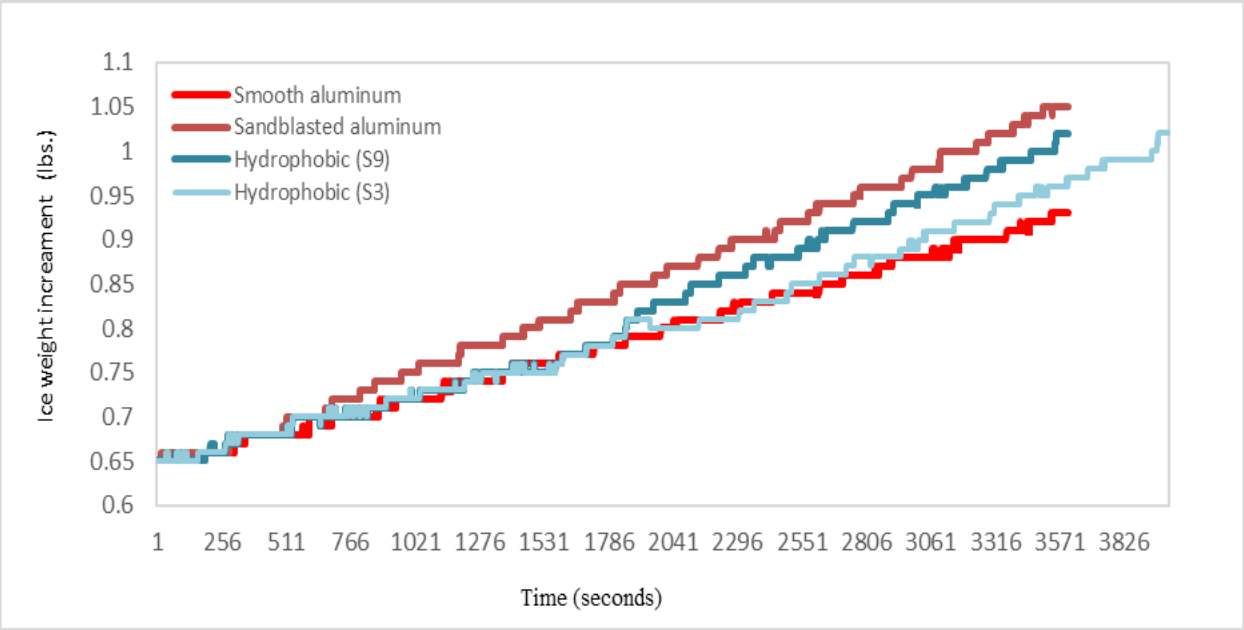

Figure 5.2. Ice accumulation weight increase data of hydrophobic coatings

5.2.3 Superhydrophobic coating ice accumulation performance

Low modulus (S3) and high modulus (S9) superhydrophobic silicone coatings ice accumulation test results were plotted against smooth aluminum and sandblasted aluminum surface. The ice weight increase test results are reported in figure 5.3. The ice weight increase of superhydrophobic coatings resulted in significantly less ice accumulation as compare to smooth and sandblasted aluminum surfaces. The primary reason for the less ice weight increase was due to significant difference in water contact angle between smooth aluminum sheet (63.7 ± 2.2), low modulus superhydrophobic coating (155.1 ± 2.1) and higher modulus superhydrophobic coating (158.5 ± 4.1), wherein superhydrophobic water contact angles helps to delay the ice nucleation and ice accretion [11,15,36 and 98].

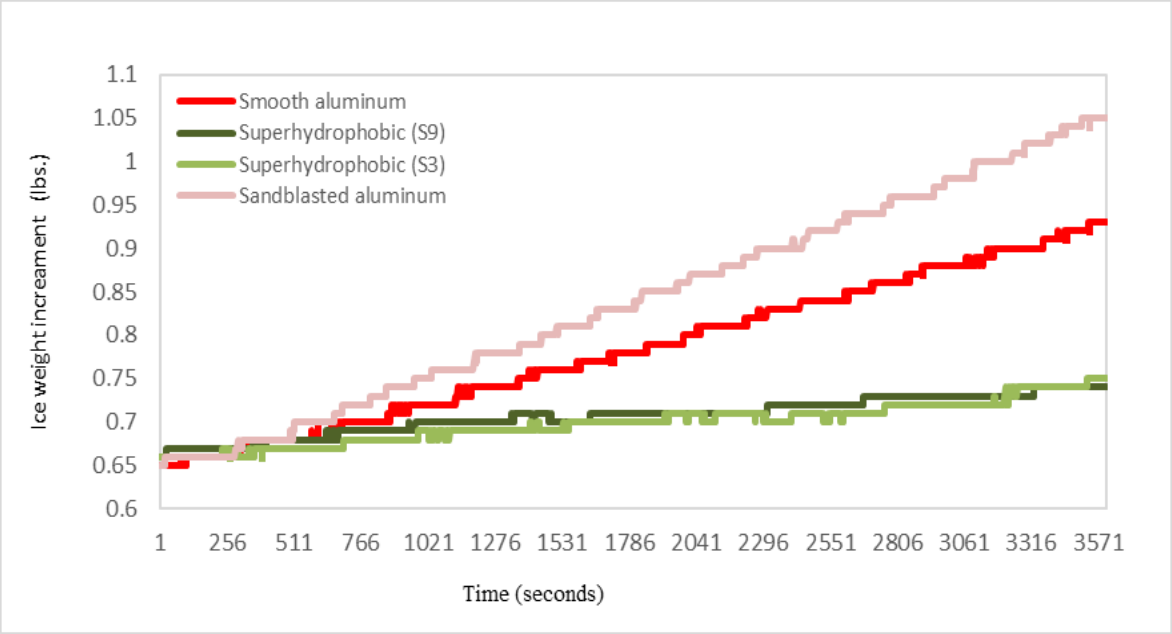

Figure 5.3. Ice accumulation weight increase data of superhydrophobic coatings

5.2.4 Low modulus coatings ice accumulation comparison

The low modulus silicone coatings (S3) ice accumulation results are plotted in the figure 5.4 and compared with uncoated smooth and sandblasted aluminum surfaces. As discussed in the previous session, superhydrophobic coating surface had accumulated less ice than other test panels. Secondly, hydrophobic and smooth aluminum surface had accumulated relatively less ice weight. The hydrophilic and sandblasted aluminum surfaces were accumulated more ice. Hydrophilic coating had highest ice accumulation because of relatively low contact angle (71.2 ± 1.3). Also, it is observed that hydrophilic silicone coatings ice accumulation was increased rapidly at initial stage (511 to 1021 seconds) of the icing process, due to that hydrophilic coating has the higher water and substrate contact area, which leads to faster ice nucleation and eventually in ice accretion [16 and 99].

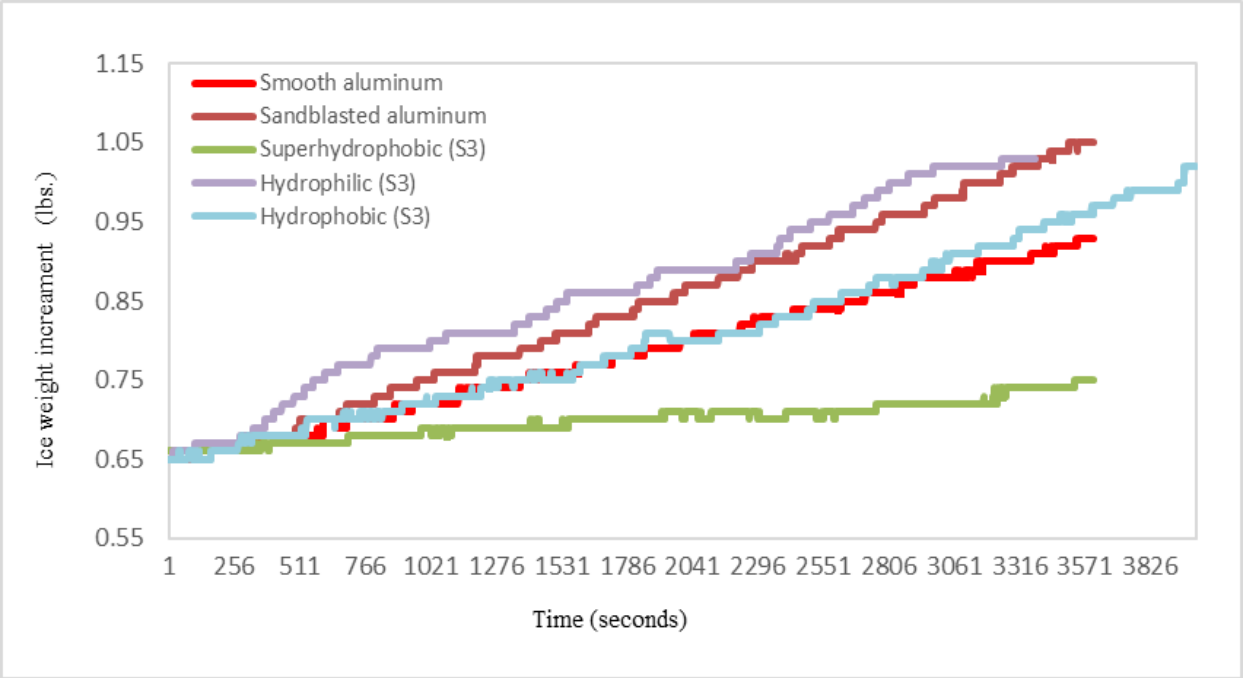

Figure 5.4. Ice accumulation weight increase data of low modulus (23 psi) coatings

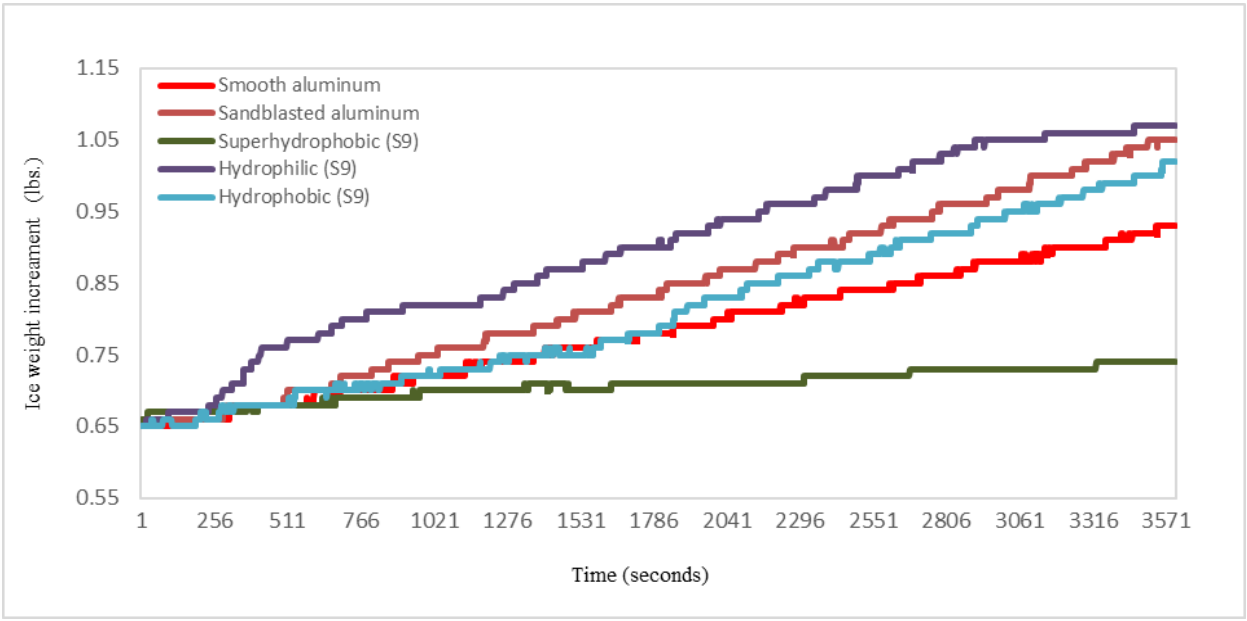

Figure 5.5. Ice accumulation weight increase data of high modulus (288 psi) coatings

5.2.5 High modulus coatings ice accumulation comparison

The high modulus silicone coatings (S9) ice accumulation results are plotted in the figure 5.5 and compared with uncoated smooth and sandblasted aluminum surface. As similar observation to low modulus coatings, high modulus superhydrophobic coating had accumulated less ice and hydrophilic silicone coating had a highest ice accumulation weight increase. Also, high modulus hydrophilic coating accreted ice more rapidly at early stage (256 seconds to 1021 seconds) of accumulation test itself. Other test panels such as high modulus hydrophobic, sandblasted and smooth aluminum ice accumulation weight increase were between earlier mentioned test samples.

5.2.6 Role of superhydrophobic test panel placement angle against water spray direction

Evaluating icephobic performance and ice accumulation of uncoated and coated aluminum test panels can provide valuable information about its influence parameters such as modulus, water contact angle and surface roughness. However exterior applications, ice accumulation can also be influenced by various other parameters such as product design, wind condition, water falling angle, water temperature and humidity. Multiple research studies have studied the role of substrate temperature, humidity and wind conditions [100 and 101]. However, very limited research work has been done regard to product design and water falling direction to the substrate surface. To understand the sample placement angle against the water spray direction, we have selected high modulus (S9) superhydrophobic test panel, since it had a very less ice accumulation.

As like previous test, water was sprayed from the top of the chamber, however the test panel placement angles were varied by tilting test panel to 0^{o} or 180^{o}, 45^{o}, 60^{o} and 90^{o} for each test. The ice accumulation test results are reported in figure 5.6.

The ice weight increase of test panels placed at the angles of 60^{o} and 90^{o} has resulted in low ice accumulation weight increase as compare to test panels were tested at the angles of 0^{o} or

180º and 45º. Interestingly, test panel placed at 90º angle had accumulated lowest ice at the early stage of accumulation process (until 3000 seconds), however, after that the increment in ice weight was similar to test panel placed at angle at 60º. It was witnessed that the ice accumulation happened at the both sides of the test panel for 90 º (since water sprayed from the top) and had contributed to the ice weight increase at the final stage of the ice accumulation test.

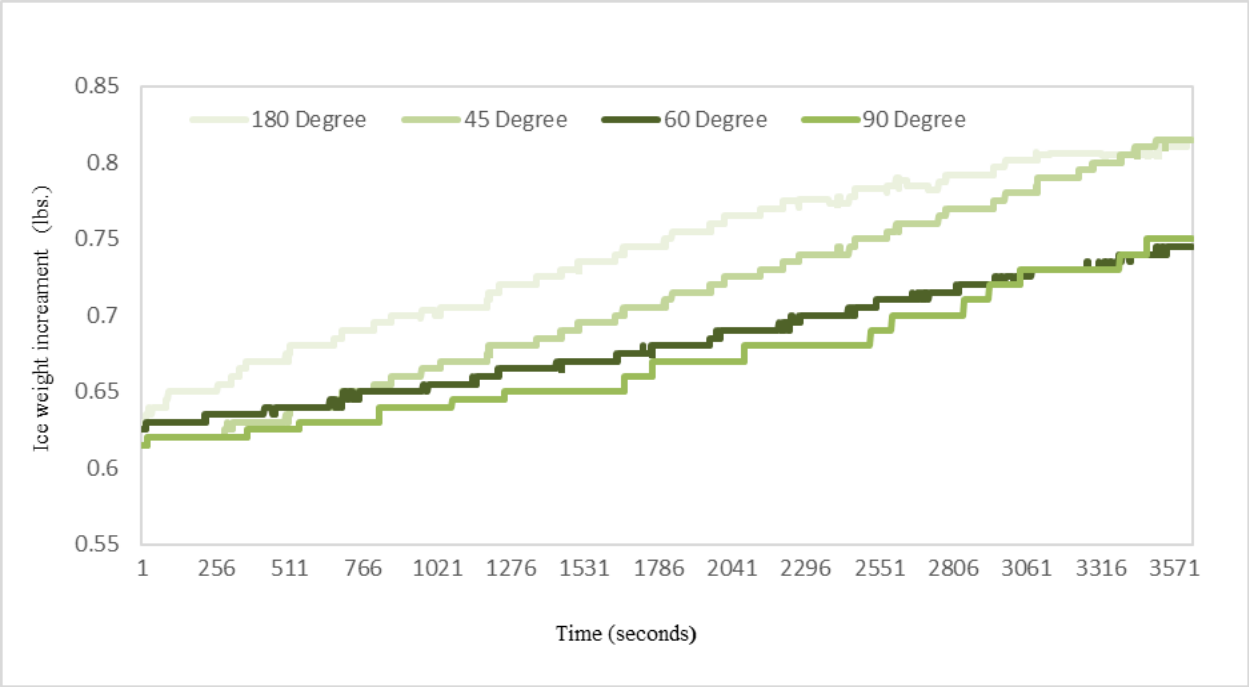

Figure 5.6. Ice accumulation weight increment of different sample placement angle (180º , 45º, 60º and 90º) against water spray direction

The sample placed at the 180º angle had highest ice accumulation as compare to all other test panels. Since, the water sliding angle of the superhydrophobic coating (7.2 ± 1.8) is higher than test panel placement angle (0º or 180º), the delay in water removal from the test panel surface had contributed to the earlier ice nucleation and ice forming process as compare to other test panels [16, 19, 98, 99 and100]. It also need to be noted that placement angle at 180º had a high surface area which is directly exposed to the water to spray, without any slop.

Interestingly, if we compare ice accumulation weight increase of smooth uncoated aluminum panel placed at 60^{o} angle (refer figure 5.7 and 5.8) to the superhydrophobic high modulus silicone test panel placed at 180^{o} angle, both had almost same ice weight increase. This finding and insight is highly valuable for product designers, though the test surface is superhydrophobic, if placement angle is not selected properly, the superhydrophobic benefit may not be realized in the final application. Additionally, product shape itself can create a difference in ice nucleation and accretion process [99 and100].

We further analyzed time taken to accumulate 0.05 lbs. of ice weight, the superhydrophobic coating ice weight with varying angle sample placement are reported in figure 5.7 and all the coatings ice weight increment measured at 60-degree angle is reported in figure 5.8. These test results suggest that sample placement is also highly critical to obtain less ice accumulation as compared to creating less ice accumulation surface itself. For example, from figure 5.7, the sample placed at 180-degree angle has accumulated 0.05 lbs. of ice in 11 minutes whereas sample placed at 60 or 90 degrees took more than 40 minutes. While comparing this data with hydrophobic or sandblasted aluminum ice accumulation data reported in figure 5.8 is almost similar time taken to accumulate 0.05 lbs. ice. This observation and learning is highly critical for product designers and developers, where product shape may influence ice accumulation.

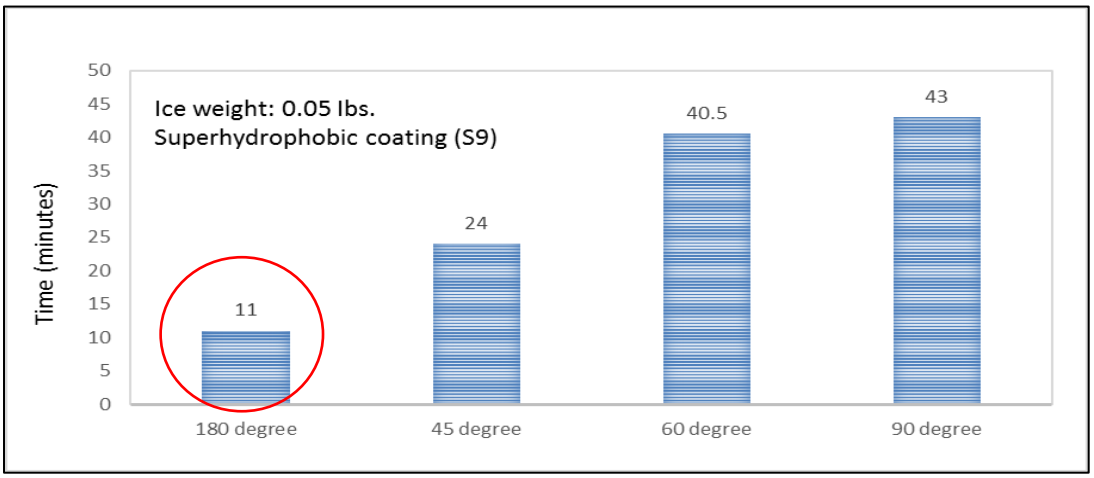

Figure 5.7. Time taken to accumulate 0.05 lbs. weight on superhydrophobic surfaces with sample placement angle (180º, 45º, 60º and 90º) against water spray direction

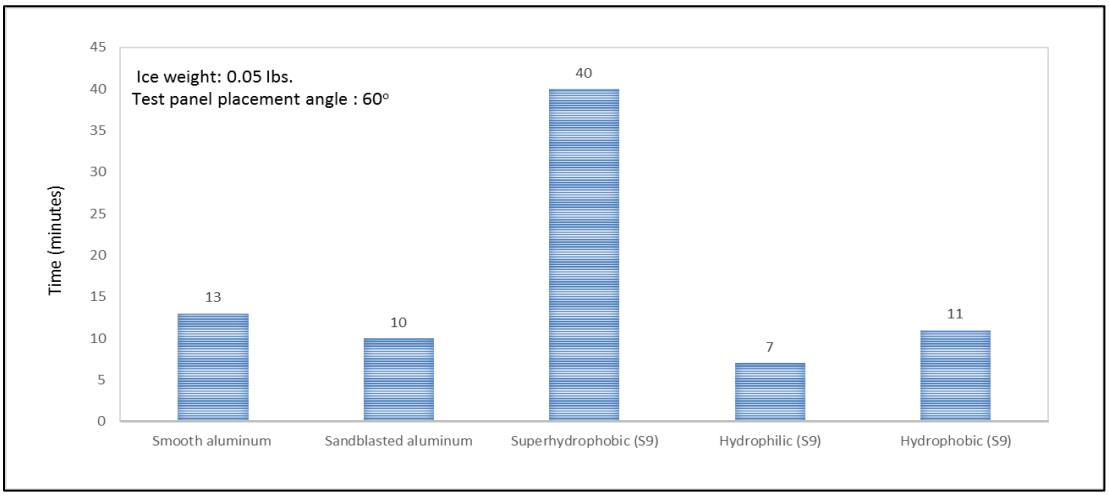

Figure 5.8. Time taken to accumulate 0.05 lbs. weight on all the test panels with sample placement angle of 60º against water spray direction

5.3 Summary and path forward

Ice weight increase of hydrophilic, hydrophobic and superhydrophobic coatings were evaluated. Hydrophilic coating resulted in higher ice weight increase and superhydrophobic coating had a lowest ice accumulation. Interestingly, uncoated smooth aluminum was performed better than hydrophilic coatings. Hydrophobic coating was resulted in moderate weight increase.

Comparatively between low modulus and high modulus hydrophilic and hydrophobic coatings, low modulus coating was accumulated less ice as compare to higher modulus coating, since soft material surface can delay ice nucleation and accretion [76, 82 and 88]. However, superhydropbic surface did not influenced by change in coating modulus.

The test panels placement angles against the water spray direction test result eludes to that though coating surface can provide better results at controlled lab environment, however actual application multiple factors need to be considered and tested before making conclusion towards icephobicity.

6. CONCLUSIONS AND FUTURE WORK

6.1 Silicone coatings icephobic performance

Silicone coating material with different characteristics attributes such as roughness (3000 GS, 300 GS and 30 GS), water contact angle (hydrophilic, hydrophobic and superhydrophobic), elastic modulus (23 psi, 88 psi, 189 psi and 288 psi) were evaluated against ice adhesion strength. The anti-ice design space plot was also established. Experimental results suggest that development of low ice adhesion strength coating is possible either with both hydrophobic and superhydrophobic coatings provided certain conditions are met. For example, if hydrophobic coating is preferred for an application scenario, the coating modulus need to be less than 100 psi. If superhydrophobic coating is selected for an application, then durability of coating need to be considered specific to the application. Moreover, we developed low ice adhesion mechanism without additional of any oil infusion to the polymer.

Silicone coating ice accumulation weight increase was measured. Superhydrophobic coating ice weight increase was less as compare to other coatings. However, appropriate design consideration need to be done during product design, since superhydrophobic coating ice accumulation can be affected by product shape and surface slop angles.

6.2 FEVE binder icephobic performance

FEVE based coating smooth and silica filled coating formulation were developed and it was compared with smooth silicone epoxy coating and superhydrophobic aerosol coatings. FEVE based smooth coating had retained its icephobic properties after high temperature ageing as compare to other benchmark coatings. Interestingly, even though superhydrophobic coating icephobic performance were better at initial unaged samples, after ageing FEVE coating retained

its surface attributes and have performed better in icephobicity. However, FEVE based smooth coating durability performance with UV, abrasion and water aging also need to be validated. Additionally, ice accumulation performance with different angle placement need to be validated in the future.

The learnings from silicone coating material evaluation and the design recommendation can be further leveraged for FEVE coating formulation, since it has higher temperature resistance and exterior weather resistance as compare to silicone coating. Low modulus FEVE based superhydrophobic coating can be a ideal solution for “durable icephobic coating for aluminum substrate”.

6.3 Opportunities for future research

Though ice adhesion and ice accumulation understanding were created. Still there are many technical unknowns need to be explored to have complete success for an industrial application. Some of them are following:

6.3.1 The role of low ice adhesion strength to product application

Researchers have demonstrated various mechanism to obtain low ice adhesion strength materials, however most of the work has been done at lab scale level only. However, actual application benefit of low ice adhesion coatings need to be validated for industrial application to increase the rate of commercial success.

6.3.2 The role of product shape in ice build-up

Ice adhesion strength were measured using flat aluminum sheet. If the low ice adhesion coating is applied on cylindrical or rectangular or “V” shaped product, would it provide the same

ice adhesion strength? Establishing this understanding would help product designers to take informed decision to consider icephobic coating for specific shape for application

6.3.3 Superhydrophobic coatings icephobic performance

Superhydrophobic coating ice accumulation was changed with sample placement angle. If certain application restricts designer to use product surface mostly with an angle of 60^{o} to water spray direction, the ice build-up would happen at the 180^{o} angle surface and continue to aggravate faster to other surfaces of the same product. So, need to validate more application related icing process to provide more insights to product designers.

REFERENCES

[1] J. Chen, K. Li, S. Wu, J. Liu, K. Liu, Q. Fan, Durable Anti-Icing Coatings Based on Self-Sustainable Lubricating Layer, ACS Omega. 2 (2017) 2047–2054. doi:10.1021/acsomega.7b00359.

[2] M. Nosonovsky, V. Hejazi, Why Superhydrophobic Surfaces Are Not always Icephobic American Chemical Society, Vol.10 (2012) 8488–8491.

[3] K.K. Varanasi, T. Deng, J.D. Smith, M. Hsu, N. Bate, Frost formation and ice adhesion on superhydrophobic surfaces, Appl. Phys. Lett. 97 (2010) 126–129. doi:10.1063/1.3524513.

[4] S. Tarquini, C. Antonini, A. Amirfazli, M. Marengo, J. Palacios, Investigation of ice shedding properties of superhydrophobic coatings on helicopter blades, Cold Reg. Sci. Technol. 100 (2014) 50–58. doi:10.1016/j.coldregions.2013.12.009.

[5] S.A. Kulinich, M. Farzaneh, On ice-releasing properties of rough hydrophobic coatings, Cold Reg. Sci. Technol. 65 (2011) 60–64. doi:10.1016/j.coldregions.2010.01.001.

[6] S. Jung, M. Dorrestijn, D. Raps, A. Das, C.M. Megaridis, D. Poulikakos, Are superhydrophobic surfaces best for icephobicity? Langmuir. 27 (2011) 3059–3066. doi:10.1021/la104762g.

[7] A.N. Zen Yoshimitsu Toshiya Watanabe, and Kazuhito Hashimoto, Effects of Surface Structure on the Hydrophobicity and Sliding Behavior of Water Droplets, Langmuir. 18 (2002) 5818–5822. doi:10.1021/la020088p.

[8] A.K. Epstein, T.-S. Wong, R.A. Belisle, E.M. Boggs, J. Aizenberg, From the Cover: Liquid-infused structured surfaces with exceptional anti-biofouling performance, Proc. Natl. Acad. Sci. 109 (2012) 13182–13187.

[9] P. Zhang, F.Y. Lv, A review of the recent advances in superhydrophobic surfaces and the emerging energy-related applications, Energy. 82 (2015) 1068–1087. doi:10.1016/j.energy.2015.01.061.

[10] X. Wei, Z. Jia, Z. Sun, M. Farzaneh, Z. Guan, Effect of the Parameters of the Semiconductive Coating on the Anti-Icing Performance of the Insulators, IEEE Trans. Power Deliv. 31 (2016) 1413–1421. doi:10.1109/TPWRD.2014.2337012.

[11] F. Wang, C. Li, Y. Lv, Y. Du, Reducing ice accumulation on aluminum conductor by applying superhydrophobic coating, Annu. Rep. - Conf. Electr. Insul. Dielectr. Phenomena, CEIDP. (2009) 311–314. doi:10.1109/CEIDP.2009.5377882.

[12] X. Wei, Z. Jia, Z. Sun, Z. Guan, M. Macalpine, Development of anti-icing coatings applied to insulators in China, IEEE Electr. Insul. Mag. 30 (2014) 42–50. doi:10.1109/MEI.2014.6749572.

[13] R. Yu, A.M. Jacobi, Self-healing , Slippery Surfaces for HVAC & R Systems, Int. Refrig. Air Cond. Conf. (2014).

[14] J. Chen, J. Liu, M. He, K. Li, D. Cui, Q. Zhang, X. Zeng, Y. Zhang, J. Wang, Y. Song, Superhydrophobic surfaces cannot reduce ice adhesion, Appl. Phys. Lett. 101 (2012) 2010–2013. doi:10.1063/1.4752436.

[15] Z. Zuo, R. Liao, C. Guo, Y. Yuan, X. Zhao, A. Zhuang, Y.Y. Zhang, Fabrication and anti-icing property of coral-like superhydrophobic aluminum surface, Appl. Surf. Sci. 331 (2015) 132–139. doi:10.1016/j.apsusc.2015.01.066.

[16] T. Bharathidasan, S.V. Kumar, M.S. Bobji, R.P.S. Chakradhar, B.J. Basu, Effect of wettability and surface roughness on ice-adhesion strength of hydrophilic, hydrophobic and superhydrophobic surfaces, Appl. Surf. Sci. 314 (2014) 241–250. doi:10.1016/j.apsusc.2014.06.101.

[17] V. Hejazi, K. Sobolev, M. Nosonovsky, From superhydrophobicity to icephobicity: forces and interaction analysis., Sci. Rep. 3 (2013) 2194. doi:10.1038/srep02194.

[18] J. Hu, K. Xu, Y. Wu, B. Lan, X. Jiang, L. Shu, The freezing process of continuously sprayed water droplets on the superhydrophobic silicone acrylate resin coating surface, Appl. Surf. Sci. 317 (2014) 534–544. doi:10.1016/j.apsusc.2014.08.145.

[19] S. Farhadi, M. Farzaneh, S. Simard, On Stability and Ice-Releasing Performance of Nanostructured Fluoro-Alkylsilane-Based Superhydrophobic Al alloy2024 Surfaces, Int. J. Theor. Appl. Nanotechnol. 1 (2012). doi:10.11159/ijtan.2012.006.

[20] J. Genzer, K. Efimenko, Recent developments in superhydrophobic surfaces and their relevance to marine fouling: A review, Biofouling. 22 (2006) 339–360. doi:10.1080/08927010600980223.

[21] L. Gao, Y. Lu, X. Zhan, J. Li, Q. Sun, A robust, anti-acid, and high-temperature-humidity-resistant superhydrophobic surface of wood based on a modified TiO2 film by fluoroalkyl silane, Surf. Coatings Technol. 262 (2015) 33–39. doi:10.1016/j.surfcoat.2014.12.005.

[22] Z. Lu, P. Wang, D. Zhang, Super-hydrophobic film fabricated on aluminium surface as a barrier to atmospheric corrosion in a marine environment, Corros. Sci. 91 (2015) 287–296. doi:10.1016/j.corsci.2014.11.029.

[23] D. Gao, M. Jia, Hierarchical ZnO particles grafting by fluorocarbon polymer derivative: Preparation and superhydrophobic behavior, Appl. Surf. Sci. 343 (2015) 172–180. doi:10.1016/j.apsusc.2015.03.024.

[24] P. Wang, D. Zhang, Z. Lu, Advantage of super-hydrophobic surface as a barrier against atmospheric corrosion induced by salt deliquescence, Corros. Sci. 90 (2015) 23–32. doi:10.1016/j.corsci.2014.09.001.

[25] L. Xiao, J. Li, S. Mieszkin, A. Di Fino, A.S. Clare, M.E. Callow, J.A. Callow, M. Grunze, A. Rosenhahn, P.A. Levkin, Slippery liquid-infused porous surfaces showing marine antibiofouling properties, ACS Appl. Mater. Interfaces. 5 (2013) 10074–10080.

[26] S. Yang, Q. Xia, L. Zhu, J. Xue, Q. Wang, Q.M. Chen, Research on the icephobic properties of fluoropolymer-based materials, Appl. Surf. Sci. 257 (2011) 4956–4962. doi:10.1016/j.apsusc.2011.01.003.

[27] R. Narayan, D.K. Chattopadhyay, B. Sreedhar, K.V.S.N. Raju, N.N. Mallikarjuna, T.M. Aminabhavi, Degradation profiles of polyester-urethane (HP-MDI) and polyester-melamine (HP-HMMM) coatings: A thermal study, J. Appl. Polym. Sci. 97 (2005) 518–526. doi:10.1002/app.21770.

[28] G. Momen, F. Madidi, M. Farzaneh, A one-step process to fabricate superhydrophobic nanocomposite coating, Icns4.Nanosharif.Ir. (2012) 12–14. http://icns4.nanosharif.ir/proceedings/files/proceedings/SYN110.pdf.

[29] X. Li, Y. Zhao, H. Li, X. Yuan, Preparation and icephobic properties of polymethyltrifluoropropylsiloxane-polyacrylate block copolymers, Appl. Surf. Sci. 316 (2014) 222–231. doi:10.1016/j.apsusc.2014.07.097.

[30] N. Valipour M., F.C. Birjandi, J. Sargolzaei, Super-non-wettable surfaces: A review, Colloids Surfaces A Physicochem. Eng. Asp. 448 (2014) 93–106. doi:10.1016/j.colsurfa.2014.02.016.

[31] G. Momen, M. Farzaneh, Simple process to fabricate a superhydrophobic coating, Micro Nano Lett. 6 (2011) 405. doi:10.1049/mnl.2011.0222.

[32] A. Irzh, L. Ghindes, A. Gedanken, Rapid deposition of transparent super-hydrophobic layers on various surfaces using microwave plasma, ACS Appl. Mater. Interfaces. 3 (2011) 4566–4572. doi:10.1021/am201181r.

[33] T.I. Gorbunova, A.Y. Zapevalov, I. V. Beketov, T.M. Demina, O.R. Timoshenkova, A.M. Murzakaev, V.S. Gaviko, A.P. Safronov, V.I. Saloutin, Preparation and antifrictional properties of surface modified hybrid fluorine-containing silica particles, Appl. Surf. Sci. 326 (2015) 19–26. doi:10.1016/j.apsusc.2014.11.091.

[34] S.M. Rao, The Effectiveness of Silane and Siloxane Treatments on the Superhydrophobicity and Icephobicity of Concrete Surfaces, (2013).

[35] A.Y. Vorobyev, C. Guo, Multifunctional surfaces produced by femtosecond laser pulses, J. Appl. Phys. 117 (2015). doi:10.1063/1.4905616.

[36] C. Antonini, M. Innocenti, T. Horn, M. Marengo, A. Amirfazli, Understanding the effect of superhydrophobic coatings on energy reduction in anti-icing systems, Cold Reg. Sci. Technol. 67 (2011) 58–67. doi:10.1016/j.coldregions.2011.02.006.

[37] K. Matsumoto, T. Sakaguchi, D. Tsubaki, H. Kubota, K. Minamiya, K. Sekine, Investigation on characteristics of thin films made from two kinds of silane-couplers to control adhesion force of ice to solid surfaces, Int. J. Refrig. 53 (2015) 177–183. doi:10.1016/j.ijrefrig.2015.01.012.

[38] Jeffrey Youngblood, John Howarter, Sathish Kumar Raganathan, Understanding Sathish, in: Underst. Role Ice Adhes. Force Influ. Ice Layer Cohes. Ice Accretion, Adhesion Society, 40th Annual Meeting, St.Petersburg, FL, 2017.

[39] K. Golovin, A. Tuteja, A predictive framework for the design and fabrication of icephobic polymers, Sci. Adv. 3 (2017) 1–10. doi:10.1126/sciadv.1701617.

[40] C. Tao, X. Li, B. Liu, K. Zhang, Y. Zhao, K. Zhu, X. Yuan, Highly icephobic properties on slippery surfaces formed from polysiloxane and fluorinated POSS, Prog. Org. Coatings. 103 (2017) 48–59. doi:10.1016/j.porgcoat.2016.11.018. [0]

[41] A.J. Meuler, J.D. Smith, K.K. Varanasi, J.M. Mabry, G.H. McKinley, R.E. Cohen, Relationships between water wettability and ice adhesion, ACS Appl. Mater. Interfaces. 2 (2010) 3100–3110. doi:10.1021/am1006035.

[42] X. Chen, R. Ma, H. Zhou, X. Zhou, L. Che, S. Yao, Z. Wang, Activating the microscale edge effect in a hierarchical surface for frosting suppression and defrosting promotion., Sci. Rep. 3 (2013) 2515. doi:10.1038/srep02515.

[43] J. Li, T. Kleintschek, A. Rieder, Y. Cheng, T. Baumbach, U. Obst, T. Schwartz, P.A. Levkin, Hydrophobic liquid-infused porous polymer surfaces for antibacterial applications, ACS Appl. Mater. Interfaces. 5 (2013) 6704–6711.

[44] P. Kim, T.S. Wong, J. Alvarenga, M.J. Kreder, W.E. Adorno-Martinez, J. Aizenberg, Liquid-infused nanostructured surfaces with extreme anti-ice and anti-frost performance, ACS Nano. 6 (2012) 6569–6577.

[45] P.W. Wilson, W. Lu, H. Xu, P. Kim, M.J. Kreder, J. Alvarenga, J. Aizenberg, Inhibition of ice nucleation by slippery liquid-infused porous surfaces (SLIPS)., Phys. Chem. Chem. Phys. 15 (2013) 581–5. http://www.ncbi.nlm.nih.gov/pubmed/23183624.

[46] M. Susoff, K. Siegmann, C. Pfaffenroth, M. Hirayama, Evaluation of icephobic coatings - Screening of different coatings and influence of roughness, Appl. Surf. Sci. 282 (2013) 870–879.

[47] D.L. Beemer, W. Wang, A.K. Kota, Durable gels with ultra-low adhesion to ice, J. Mater. Chem. A. (2016). doi:10.1039/c6ta07262c.

[48] J.D. Brassard, J.L. Laforte, C. Blackburn, J. Perron, D.K. Sarkar, Silicone based superhydrophobic coating efficient to reduce ice adhesion and accumulation on aluminum under offshore arctic conditions, Ocean Eng. (2017). doi:10.1016/j.oceaneng.2017.08.022.

[49] Z. He, S. Xiao, H. Gao, J. He, Z. Zhang, Multiscale crack initiator promoted super-low ice adhesion surfaces, Soft Matter. (2017). doi:10.1039/c7sm01511a.

[50] J.D. Brassard, D.K. Sarkar, J. Perron, A. Audibert-Hayet, D. Melot, Nano-micro structured superhydrophobic zinc coating on steel for prevention of corrosion and ice adhesion, J. Colloid Interface Sci. (2014). doi:10.1016/j.jcis.2014.11.076.

[51] Z. He, Y. Zhuo, J. He, Z. Zhang, Design and preparation of sandwich-like polydimethylsiloxane (PDMS) sponges with super-low ice adhesion, Soft Matter. (2018). doi:10.1039/c8sm00820e.

[52] K. Viswanathan, N.K. Sundaram, S. Chandrasekar, Stick-slip at soft adhesive interfaces mediated by slow frictional waves, Soft Matter. (2016). doi:10.1039/c6sm00244g.

[52] Y. Shen, H. Tao, S. Chen, L. Zhu, T. Wang, J. Tao, Icephobic/anti-icing potential of superhydrophobic Ti6Al4V surfaces with hierarchical textures, RSC Adv. 5 (2015) 1666–1672. doi:10.1039/C4RA12150C.

[53] M. Nosonovsky, V. Hejazi, Why superhydrophobic surfaces are not always icephobic, ACS Nano. 6 (2012) 8488–8491. doi:10.1021/nn302138r.

[54] Meuler AJ1, Smith JD, Varanasi KK, Mabry JM, McKinley GH, Cohen RE. Relationships between water wettability and ice adhesion; ACS Appl Mater Interfaces. 2010 Nov;2(11):3100-10. doi: 10.1021/am1006035.

[55] L. Oberli, D. Caruso, C. Hall, M. Fabretto, P.J. Murphy, D. Evans, Condensation and freezing of droplets on superhydrophobic surfaces, Adv. Colloid Interface Sci. 210 (2014) 47–57. doi:10.1016/j.cis.2013.10.018.

[56] L. Cao, A.K. Jones, V.K. Sikka, J. Wu, D. Gao, Anti-Icing superhydrophobic coatings, Langmuir. 25 (2009) 12444–12448. doi:10.1021/la902882b.

[57] M. Zou, S. Beckford, R. Wei, C. Ellis, G. Hatton, M.A. Miller, Effects of surface roughness and energy on ice adhesion strength, Appl. Surf. Sci. 257 (2011) 3786–3792. doi:10.1016/j.apsusc.2010.11.149.

[58] K Kendall, The adhesion and surface energy of elastic solids; Journal of Physics D: Applied Physics, Volume 4, Number 8

[59] Brady, R. F.; Singer, I. L. Mechanical factors favoring release from fouling release coatings. Biofouling 2000, 15 (1-3), 73-81.

[60] Per-Olof Glantz & Robert E. Baier, Recent Studies on Nonspecific Aspects of Interfacial

Adhesion (1986)

[61] Vladkova, Surface Engineering for Non-toxic Biofouling Control;; 239; Journal of the University of Chemical Technology and Metallurgy, 42, 3, 2007, 239-256

[62] Jeffrey Youngblood, John Howarter, Sathish Kumar Raganathan, Moving antiice, in: Mov. Anti-Ice Coatings from Lab to F. Key Issues to Overcome Fluoropolymer Coatings, Fluoropolymer coatings, New Orleans, LA, 2016.

[63] K.N. Allahar, D. Battocchi, G. Bierwagen, D. Tallman, Thermal Degradation of a Mg-Rich Primer on AA 2024-T3, 19 (2009) 75–89. doi:10.1149/1.3259800.

[64] D.H. Lee, K. Golovin, E.T. DiLoreto, J.M. Mabry, A. Tuteja, S.P.R. Kobaku, Designing durable icephobic surfaces, Sci. Adv. 2 (2016) e1501496. doi:10.1126/sciadv.1501496.

[65] X. Wu, X. Zhao, J.W.C. Ho, Z. Chen, Design and durability study of environmental-friendly room-temperature processable icephobic coatings, Chem. Eng. J. (2019). doi:10.1016/j.cej.2018.07.204.

[66] L.B. Boinovich, A.M. Emelyanenko, V.K. Ivanov, A.S. Pashinin, Durable icephobic coating for stainless steel, ACS Appl. Mater. Interfaces. (2013). doi:10.1021/am3031272.

[67] W. Darden, Ultra Weatherable Fluoropolymer Coatings For Bridges, in: Maint. Roadw. Oper. Work., Kansas City, Missouri, n.d.

[68] S. Munekata, Fluoropolymers as coating material, Prog. Org. Coatings. 16 (1988) 113–134. doi:10.1016/0033-0655(88)80010-4.

[69] A. Fallis, Lumiflon Fluoropolymer Resins Long Term Performance Vs. PVDF, J. Chem. Inf. Model. (2013). doi:10.1017/CBO9781107415324.004.

[70] LUMIFLON FEVE resins provide color retention, corrosion resistance to auto coatings, Focus Powder Coatings. (2016). doi:10.1016/j.fopow.2016.08.024.

[71] L. Li, X.C. Guo, Y.Y. Zhou, The Research of Chemical Resistance for Air Curing FEVE Fluorocarbon Coatings, Adv. Mater. Res. 239–242 (2011) 944–948. doi:10.4028/www.scientific.net/AMR.239-242.944.

[72] J. Li, Y. Zhao, J. Hu, L. Shu, X. Shi, Anti-icing performance of a superhydrophobic PDMS/modified nano-silica hybrid coating for insulators, J. Adhes. Sci. Technol. (2012). doi:10.1163/016942411X574826.

[73] B.K. Lee, J.H. Ryu, I.B. Baek, Y. Kim, W.I. Jang, S.H. Kim, Y.S. Yoon, S.H. Kim, S.G. Hong, S. Byun, H.Y. Yu, Silicone-Based Adhesives with Highly Tunable Adhesion Force for Skin-Contact Applications, Adv. Healthc. Mater. (2017). doi:10.1002/adhm.201700621.

[74] A.M. Emelyanenko, L.B. Boinovich, A.A. Bezdomnikov, E. V. Chulkova, K.A. Emelyanenko, Reinforced Superhydrophobic Coating on Silicone Rubber for Longstanding Anti-Icing Performance in Severe Conditions, ACS Appl. Mater. Interfaces. (2017). doi:10.1021/acsami.7b05549.

[75] K. Qiang Zhang, J. zhe Cai, X. hui Li, H. Li, Y. hui Zhao, X. yan Yuan, Balance of polyacrylate-fluorosilicone block copolymers as icephobic coatings, Chinese J. Polym. Sci. (English Ed. 33 (2015) 153–162. doi:10.1007/s10118-015-1563-9.

[76] J. Chen, W. Wang, Analytical Study on Wind-induced Vibration of Ice Coating Transmission Line Systems, Manuf. Sci. Technol. Pts 1-8. 383–390 (2012) 3657–3662. doi:10.4028/www.scientific.net/AMR.383-390.3657.

[77] L. Zhu, J. Xue, Y. Wang, Q. Chen, J. Ding, Q. Wang, Ice-phobic coatings based on silicon-oil-infused polydimethylsiloxane, ACS Appl. Mater. Interfaces. (2013). doi:10.1021/am400704z.

[78] Y. Liu, L. Ma, W. Wang, A.K. Kota, H. Hu, An experimental study on soft PDMS materials for aircraft icing mitigation, Appl. Surf. Sci. (2018). doi:10.1016/j.apsusc.2018.04.032.

[79] J. Wei, B. Di, L. Wang, P. Ding, Physical model experimental research on the impact of crack density on fast shear wave and slow shear wave velocities, Geophys. Prospect. Pet. (2014). doi:10.3969/j.issn.1000-1441.2014.03.001.

[80] L. Makkonen, Ice adhesion - Theory, measurements and countermeasures, J. Adhes. Sci. Technol. 26 (2012) 413–445. doi:10.1163/016942411X574583.

[81] Y. Kwon, S. Choi, N. Anantharaju, J. Lee, M. V. Panchagnula, N.A. Patankar, Is the Cassie-Baxter formula relevant?, Langmuir. 26 (2010) 17528–17531. doi:10.1021/la102981e.

[82] R. Huang, C.M. Stafford, B.D. Vogt, Effect of Surface Properties on Wrinkling of Ultrathin Films, J. Aerosp. Eng. 20 (2006) 38–44. doi:10.1061/(asce)0893-1321(2007)20:1(38).

[83] O. Gohardani, The Exploration of Icephobic Materials and Their Future Prospects in Aircraft Icing Applications, J. Aeronaut. Aerosp. Eng. 01 (2012) 1–2. doi:10.4172/2168-9792.1000e116.

[84] J. Jeevahan, M. Chandrasekaran, G. Britto Joseph, R.B. Durairaj, G. Mageshwaran, Superhydrophobic surfaces: a review on fundamentals, applications, and challenges, J. Coatings Technol. Res. (2018). doi:10.1007/s11998-017-0011-x.

[85] X. Yao, Y. Hu, A. Grinthal, T.-S. Wong, L. Mahadevan, J. Aizenberg, Adaptive fluid-infused porous films with tunable transparency and wettability., Nat. Mater. 12 (2013) 529–34. http://www.ncbi.nlm.nih.gov/pubmed/23563739.

[86] P. Kim, M.J. Kreder, J. Alvarenga, J. Aizenberg, Hierarchical or not? Effect of the length scale and hierarchy of the surface roughness on omniphobicity of lubricant-infused substrates, Nano Lett. 13 (2013) 1793–1799.

[87] Z. He, E.T. Vågenes, C. Delabahan, J. He, Z. Zhang, Room Temperature Characteristics of Polymer-Based Low Ice Adhesion Surfaces, Sci. Rep. (2017). doi:10.1038/srep42181.

[88] L. Xue, J.T. Pham, J. Iturri, A. Del Campo, Stick-Slip Friction of PDMS Surfaces for Bioinspired Adhesives, Langmuir. (2016). doi:10.1021/acs.langmuir.6b00513.

[89] C. Bukowsky, J.M. Torres, B.D. Vogt, Slip-stick wetting and large contact angle hysteresis on wrinkled surfaces, J. Colloid Interface Sci. (2011). doi:10.1016/j.jcis.2010.11.034.

[90] K. Viswanathan, N.K. Sundaram, S. Chandrasekar, Slow wave propagation in soft adhesive interfaces, Soft Matter. (2016). doi:10.1039/C6SM01960A.

[91] P.E. Mallon, Y. Li, R. Zhang, H. Chen, Y. Wu, T.C. Sandreczki, Y.C. Jean, R. Suzuki, T. Ohdaira, Durability of polymeric coatings: Effects of natural and artificial weathering, Appl. Surf. Sci. 194 (2002) 176–181. doi:10.1016/S0169-4332(02)00120-4.

[92] Z.A. Janjua, B. Turnbull, K.L. Choy, C. Pandis, J. Liu, X. Hou, K.S. Choi, Performance and durability tests of smart icephobic coatings to reduce ice adhesion, Appl. Surf. Sci. 407 (2017) 555–564. doi:10.1016/j.apsusc.2017.02.206.

[93] M.J. Kreder, J. Alvarenga, P. Kim, J. Aizenberg, Design of anti-icing surfaces: Smooth, textured or slippery?, Nat. Rev. Mater. (2016). doi:10.1038/natrevmats.2015.3.

[94] H.B. Eral, D.J.C.M. 'T Mannetje, J.M. Oh, Contact angle hysteresis: A review of fundamentals and applications, Colloid Polym. Sci. 291 (2013) 247–260. doi:10.1007/s00396-012-2796-6.

[95] N. Cohen, A. Dotan, H. Dodiuk, S. Kenig, Superhydrophobic Coatings and Their Durability, Mater. Manuf. Process. (2016). doi:10.1080/10426914.2015.1090600.

[96] J.B. Boreyko, B.R. Srijanto, T.D. Nguyen, C. Vega, M. Fuentes-Cabrera, C.P. Collier, Dynamic defrosting on nanostructured superhydrophobic surfaces, Langmuir. 29 (2013) 9516–9524. doi:10.1021/la401282c.

[97] N. Srikanth, E. Liu, P. Wilson, Z. Chen, Development of Sol − Gel Icephobic Coatings: Effect of Surface Roughness and Surface Energy, Appl. Mater. Interfaces. (2014).

[98] N. Miljkovic, R. Enright, Y. Nam, K. Lopez, N. Dou, J. Sack, E.N. Wang, Jumping-Droplet-Enhanced Condensation on Scalable Superhydrophobic Nanostructured Surfaces, (2012).

[99] W.D. Bascom, R.L. Cottington, C.R. Singleterry, Ice Adhesion to Hydrophilic and Hydrophobic Surfaces, J. Adhes. (1969). doi:10.1080/00218466908072188.

[100] Z. Jin, S. Jin, Z. Yang, An experimental investigation into the icing and melting process of a water droplet impinging onto a superhydrophobic surface, Sci. China Physics, Mech. Astron. 56 (2013) 2047–2053. doi:10.1007/s11433-013-5209-z

[101] J.J. Petrovic, Mechanical properties of ice and snow, J. Mater. Sci. (2003). doi:10.1023/A:1021134128038.

VITA

Sathish Kumar Ranganathan was born in Cuddalore, India. He received his B.S in Chemical Engineering from Madras University and M.S. degree in Polymer Science and Technology from Visveswaraya University, India. He has previous work experience with General Electric Plastics, India; Mahindra & Mahindra Automotive Ltd., India; and currently working with General Cable (Prysmian group), USA since past 8 years. He then went to pursue his Ph.D. degree in Materials Engineering at Purdue University, West Lafayette, Indiana, U.S.A.

PUBLICATIONS

1. John Howarter, Sathish Kumar, Ranganathan, Jeffery Youngblood, Srinivas Siripurapu; Impacts of Thermal Cycling on Hydrophobicity and Ice Adhesion on Ice-phobic coatings for Energy Related Applications, Adhesion Society 39th Annual Meeting, 2015, FL, USA
2. Jeffery Youngblood, John Howarter , Sathish Kumar, Ranganathan, Srinivas Siripurapu; Moving Anti-ice Coatings from the Lab to the Field: Solving the Path from Curiosity to Industry, Fluoropolymer conference, 2016, New Orleans, LA USA http://polyacs.net/Workshops/16Fluoropolymer/FP/images/Speakers/pdf/38Youngblood.pdf
3. Jeffery Youngblood, Sathish Kumar, Ranganathan, John Howarter , Srinivas Siripurapu; Moving anti-ice Coatings from the lab to the field: Key issues to overcome; ACS National Meeting 2016, San Diego http://sandiego2016.acs.org/i/651144-computers-in-chemistry/280
4. Sathish Kumar, Ranganathan, Jeffery Youngblood, John Howarter, Srinivas Siripurapu; Understanding of Role of Ice Adhesion Force and Influences of Ice Layer Cohesion Forces in Ice Accretion; Adhesion Society Committee Conference, 40th Annual Meeting 2017, FL.
5. Sathish Kumar, Ranganathan, Jeffery Youngblood, John Howarter, Srinivas Siripurapu, "Development of environmentally friendly water-based coatings to resist water and ice," American Coating Tech Conference, 2017, Cleveland, OH
6. Jeffery Youngblood, John Howarter, Sathish Kumar, Ranganathan; Impacts of Thermal Cycling on Hydrophobicity and Ice Adhesion on Ice-phobic coatings for Energy Related Applications, Adhesion Society 41st Annual Meeting, March 2018, USA
7. Compositions and coatings formed thereof with reduced ice adherence and accumulation (patent publication number: 20170321077)
8. Thermally Durable Water-based Coatings: Does Smooth Coating is Better Icephobicity Than Superhydrophobic Coating? (Ready for paper submission)
9. Influence of coating properties to ice adhesion strength (under drafting)